

Copyright
by
Eric Alexander Nicholson
2018

The Dissertation Committee for Eric Alexander Nicholson
certifies that this is the approved version of the following dissertation:

**Perturbative Wilsonian Formalism for Noncommutative
Gauge Theories in the Matrix Representation**

Committee:

Willy Fischler, Supervisor

Jacques Distler

Vadim Kaplunovsky

Sonia Paban

Dan Freed

**Perturbative Wilsonian Formalism for Noncommutative
Gauge Theories in the Matrix Representation**

by

Eric Alexander Nicholson, B.S.

DISSERTATION

Presented to the Faculty of the Graduate School of
The University of Texas at Austin
in Partial Fulfillment
of the Requirements
for the Degree of

DOCTOR OF PHILOSOPHY

THE UNIVERSITY OF TEXAS AT AUSTIN

December 2018

Dedicated to my loving wife, Elizabeth, whose support has been invaluable.

Acknowledgments

I wish to thank all of the members of the Theory Group for providing a stimulating scientific environment. However, Willy Fischler and Sonia Paban are especially deserving of thanks for all of the advice and support that they have provided over the years. I would also like to thank Li Jiang for countless valuable and spirited discussions.

Perturbative Wilsonian Formalism for Noncommutative Gauge Theories in the Matrix Representation

Publication No. _____

Eric Alexander Nicholson, Ph.D.
The University of Texas at Austin, 2018

Supervisor: Willy Fischler

We study the perturbative approach to the Wilsonian integration of noncommutative gauge theories in the matrix representation. We begin by motivating the study of noncommutative gauge theories and reviewing the matrix formulation. We then systematically develop the perturbative treatment of UV states and calculate both the leading and next to leading order one- and two-loop corrections to the quantum effective action. Throughout, we discuss how our formalism clarifies problems associated with UV-IR mixing, a particular emphasis being placed on the dipole structure imposed by noncommutative gauge invariance. Ultimately, using the structural understanding developed in this work, we are able to determine the exact form of perturbative corrections in the UV regime defined by $\theta\Lambda^2 \gg 1$. Finally, we apply our results to the analysis of the divergence structure and show that 3+1 and higher dimensional noncommutative theories that allow renormalization beyond one-loop are not self-consistent.

Table of Contents

Acknowledgments	v
Abstract	vi
List of Figures	ix
Chapter 1. Introduction and Motivation	1
Chapter 2. Matrix Representation of Noncommutative Gauge Theories	6
2.1 Introduction	6
2.2 Matrix Representation of the Noncommutative Plane	6
2.3 Matrix Formulation of Noncommutative Gauge Theories	10
Chapter 3. Perturbative Wilsonian Formalism for Noncommutative Gauge Theories	
3.1 Introduction	14
3.2 Background Field Gauge Fixing	14
3.3 Propagator in the Matrix Representation	18
3.4 One-loop Corrections to the Effective Action	23
3.5 Higher Loop Corrections to the Effective Action	30
Chapter 4. Application of the Perturbative Wilsonian Formalism to the Divergences	
4.1 Introduction	37
4.2 Divergences and UV-IR Mixing	38
4.3 Treatment of UV and UV-IR Divergences	44
Chapter 5. Discussion and Outlook	53
Appendices	57
Appendix A. Orthogonality and Completeness Relations for the Fourier Matrix Basis	

Appendix B.	Propagator in the Fourier Matrix Basis	60
Appendix C.	Equivalence Between the Fourier Basis Matrices and Wilson Lines	63
Appendix D.	Next to Leading Order One-Loop Diagram	64
Appendix E.	Leading Order Two-Loop Diagrams	66
Appendix F.	Next to Leading Order Two-Loop Diagrams	70
	Bibliography	72
	Vita	75

List of Figures

- 3.1 One-loop contributions in the matrix versus the star product approach. 23
- 3.2 High momentum virtual dipoles grow long in the transverse direction and mediate instabilities. 24
- 3.3 Long distance three-body interactions corresponding to high momentum dipoles propagating in the transverse direction. 25

Chapter 1

Introduction and Motivation

The most significant outcome of purely theoretical physics in the last thirty years is string theory. String theories, which naturally live in $9 + 1$ dimensions, seem to provide a unified perturbative description of all known interactions – including gravity. In more recent years, however, it has been discovered that even string theories appear to be unified into a mysterious $10 + 1$ dimensional theory known as \mathcal{M} -theory, which is believed to exist even at the non-perturbative level.

One of the most interesting and also most challenging aspects of \mathcal{M} -theory is that it appears to admit a large number of equivalent descriptions, each with its own set of degrees of freedom and interactions. Equivalences of this type are known as *dualities*. By their very nature, dualities impose severe difficulties on the formulation of a background independent description of the theory, because some degrees of freedom are more natural in certain backgrounds but none are universally favored. Furthermore, \mathcal{M} -theory seems to incorporate a radical concept called *holography*, which requires that the number of degrees of freedom in a region of space grows as the area enclosing the region, instead of the volume. For this reason, holography also obscures

the background independence of the theory, since one must choose a particular “holographic screen” on which to “project” a description of the physics. Moreover, it is not known the extent to which duality and holography interplay in \mathcal{M} -theory.

Nonetheless, one conceivable way to formulate a theory which embodies duality or holography in a background independent fashion is to make manifest a symmetry whose action is equivalent to a duality transformation or changing the choice of holographic screen. In other words, one may choose to intentionally formulate the theory in a highly redundant language. After all, historically, this method has been proven correct in formulating gauge theories, which are somewhat analogous. From this point of view, different dual descriptions of the same physics or different choices of holographic screen are merely different (partial) gauge choices. Moreover, the reduction in degrees of freedom implied by holography would presumably arise from eliminating all (or most of) the gauge freedom. The problem is that duality and holography imply such a rich structure that it is not known how to parameterize any symmetry that could describe their full effect. Although, there has been some evidence that suggests manifestly duality invariant theories may be formulated in backgrounds with more than one time-like dimension [1].

Following this line of reasoning, the key to discovering a tractable background independent formulation of \mathcal{M} -theory may be to study nontrivial extensions of local gauge symmetry. Perhaps the most conservative step in this direction is to study noncommutative gauge theories, which are important in

their own right because they are known to emerge from string theory through various decoupling limits [2, 3]. However, in the context of the present discussion, noncommutative gauge theories could provide some clues about the nature of whatever mysterious symmetry casts \mathcal{M} -theory in its most symmetric form.

It turns out that noncommutative gauge theories do indeed contain an essential ingredient which is necessary to accommodate holography – *UV-IR mixing*. UV-IR mixing, or the UV-IR connection, refers to a nondecoupling of UV and IR degrees of freedom. Clearly, a nondecoupling of this type is required in any holographic theory because the total number of degrees of freedom in a region – a quantity dependent on the UV – is related to the area enclosing the region – a quantity dependent on the IR. In noncommutative gauge theories, UV-IR mixing arises from elementary dipole degrees of freedom whose transverse length is proportional to their center-of-mass momentum [3]. Thus, UV dipoles grow long in spatial extent and mediate instantaneous long-distance interactions that are relevant in the IR. What is more, the dipole character of noncommutative gauge theories is intimately related to the structure imposed by gauge invariance.

However, while it may be plausible that the study of noncommutative gauge invariance can shed some light on duality and holography, the main objective of this work is to probe the effects of UV-IR mixing in the context of noncommutative gauge theories. In particular, we perturbatively analyze Wilsonian integration in the UV regime defined by $\theta\Lambda^2 \gg 1$. Although not as

fundamental in nature, this problem is quite interesting and challenging due to the inherent involvement of both spatial nonlocality and UV-IR nondecoupling. In fact, both of these properties present major difficulties in the understanding of noncommutative quantum field theories.

The most popular approach to studying noncommutative field theories has been to work in the star product representation and apply the conventional techniques that were originally developed for local quantum field theories. Not surprisingly, UV-IR mixing results in a tremendous amount of confusion regarding such things as the renormalization of UV divergences [4, 5, 6], the treatment of IR divergences [7, 8], and Wilsonian integration [9, 10]. Moreover, the noncommutative gauge invariance is not preserved order by order in the standard perturbative expansion [11]. Rather, gauge invariance is achieved by an infinite resummation of diagrams [12, 13, 14]. Finally, there is a sort of naturalness problem with the conventional approach in that the intrinsic dipole structure of the elementary field quanta is not completely clear, although some suggestive results have been obtained [12].

On the other hand, in the matrix formulation of noncommutative gauge theory, the noncommutative gauge invariance is manifest [15], as is the dipole character of the elementary quanta [16, 17]. In fact, the matrix approach allows for a clear separation between the quantum effects of UV and IR dipoles. In particular, it has been shown that one can make sense of Wilsonian integration despite UV-IR mixing, and corrections to the quantum effective action resulting from integrating out the UV states were explicitly calculated at both

the one- and two-loop orders. The resulting interactions were found to dominate the long-distance behavior, which shed some light on UV-IR mixing in noncommutative gauge theory, as well as the nonanalytic dependence of the quantum theory on the noncommutativity parameter θ . Also, [18] provides a different point of view on how the matrix formulation naturally leads to a bi-local representation. Thus, the dipole structure imposed by the manifest gauge invariance of the matrix formulation seems to hold the key to resolving the ambiguities associated with UV-IR mixing.

In this work, we will review and build upon the recent developments in the perturbative approach to Wilsonian integration of noncommutative gauge theories in the matrix formulation. In Chapter 2, we discuss the matrix formulation of noncommutative gauge theories in some detail. The presentation is based on [19, 20], although the proofs of orthogonality and completeness of the Fourier matrix basis are new. Then in Chapter 3, which is essentially drawn from [16, 17], we discuss the perturbative Wilsonian treatment of noncommutative gauge theories in the UV regime given by $\theta\Lambda^2 \gg 1$. Finally, Chapter 4 addresses the divergence structure that arises from the integration of UV modes. To some extent this part is based on [17], although there are new discussions concerning diagrammatical combinatorics and the relationship between renormalization beyond one loop and UV-IR divergences. We end in Chapter 5 with some discussion of our results and outlook toward the open problem of understanding the IR regime defined by $\theta\Lambda^2 \lesssim 1$. The Appendices contain the technical details and explicit calculations.

Chapter 2

Matrix Representation of Noncommutative Gauge Theories

2.1 Introduction

Before systematically developing the perturbative Wilsonian treatment of noncommutative gauge theories in the matrix formulation, we must first discuss the matrix representation of the noncommutative plane. To that end, we will first define the noncommutative plane algebraically and then briefly discuss its novel properties. We then derive the matrix representation of functions defined on the noncommutative plane and discuss the correspondence with the star product representation. Finally, we formulate noncommutative gauge theories in the matrix representation.

2.2 Matrix Representation of the Noncommutative Plane

The noncommutative $2p$ -plane is most conveniently defined by its algebra

$$[x^i, x^j] = i\theta^{ij}, \quad (2.1)$$

where x^i are the coordinates and θ^{ij} is an antisymmetric tensor of $SO(2p)$. Clearly, the novel feature of the noncommutative plane is that the coordinates

generally do not commute. However, we may still think of the coordinates as any other observable in our Hilbert space, and therefore, represent them as infinite dimensional Hermitian matrices \hat{x}^i . The difference in the noncommutative case is that Eq. (2.1) leads to a nontrivial uncertainty relation between the coordinate operators

$$\Delta x^i \Delta x^j \gtrsim \theta^{ij}. \quad (2.2)$$

In words, Eq. (2.2) states that, on the noncommutative plane, configurations that are localized in a given direction are necessarily delocalized in the transverse direction.

Furthermore, when combined with the standard position-momentum uncertainty relation, Eq. (2.2) implies that high momentum configurations are necessarily to some extent delocalized. As we shall see in Chapter 3, these novel properties of the noncommutative plane will lead to spatial nonlocality and UV-IR nondecoupling, which poses some technical obstacles to understanding noncommutative quantum field theories. However, the matrix representation is particularly well-suited to describe this type of behavior, and will therefore be the preferred language in which to formulate noncommutative field theories.

In order to quantify the notion of “configurations” that are discussed above, we must first give a definition to arbitrary functions of noncommutative coordinates. In the matrix representation, we can think of functions defined on the noncommutative plane as matrices. Moreover, in analogy with the familiar Fourier expansion of ordinary functions, it will prove convenient to define functions of noncommutative coordinates by means of an expansion in

a special basis of matrices

$$F = \int \frac{d^{2p}k}{(2\pi)^{2p}} e^{ik \cdot \hat{x}} \tilde{F}(k). \quad (2.3)$$

When expressed this way, F is a Weyl ordered function of \hat{x}^i since the exponential is.

The validity of Eq. (2.3) follows from the orthogonality and completeness relations that are derived in Appendix A

$$(2\pi)^p (\det\theta)^{1/2} \text{Tr} \left(e^{ik \cdot \hat{x}} e^{-ik' \cdot \hat{x}} \right) = (2\pi)^{2p} \delta^{2p}(k - k') \quad (2.4)$$

$$\int \frac{d^{2p}k}{(2\pi)^{2p}} (e^{ik \cdot \hat{x}})_{ij} (e^{-ik \cdot \hat{x}})_{kl} = \frac{\delta_{il} \delta_{kj}}{(2\pi)^p (\det\theta)^{1/2}}. \quad (2.5)$$

Eqs. (2.4) and (2.5) imply that the Fourier coefficients are given by

$$\tilde{F}(k) = (2\pi)^p (\det\theta)^{1/2} \text{Tr} \left(e^{-ik \cdot \hat{x}} F \right). \quad (2.6)$$

In what is to follow, we shall *define* $f(\hat{x})$ as the matrix whose Fourier coefficients are

$$\tilde{f}(k) = \int d^{2p}x e^{-ik \cdot x} f(x). \quad (2.7)$$

Eq. (2.7) is the canonical choice because it implies that, as a function of its argument, $f(\hat{x})$ reduces to $f(x)$ in the commutative limit. However, perhaps the most convenient aspect of Eq. (2.7) is that it implies

$$(2\pi)^p (\det\theta)^{1/2} \text{Tr} f(\hat{x}) = \int d^{2p}x f(x), \quad (2.8)$$

which will play a crucial role in constructing the action for noncommutative field theories.

An immensely important consequence of Eq. (2.7) is that it immediately provides a one-to-one correspondence between matrix functions and ordinary functions

$$f(\hat{x}) \longleftrightarrow f(x). \quad (2.9)$$

Thus, to $f(\hat{x})$, we may attribute a profile in position and momentum space given by $f(x)$ and $\tilde{f}(k)$, respectively. It is, however, important to realize that there is a crucial difference between the algebra of functions defined on the noncommutative plane and those defined on the ordinary plane. For example, consider the product of two matrix functions $f(\hat{x})$ and $g(\hat{x})$. From Eqs. (2.7) and (2.9) it follows that

$$f(\hat{x})g(\hat{x}) \longleftrightarrow (f \star g)(x) \equiv \exp\left(\frac{i}{2}\partial_i\theta^{ij}\partial'_j\right) f(x)g(x') \Big|_{x'=x}. \quad (2.10)$$

Thus, if we choose to represent the matrix functions $f(\hat{x})$ and $g(\hat{x})$ by the ordinary functions $f(x)$ and $g(x)$, we must deform the ordinary product into the star product as shown in Eq. (2.10). This choice corresponds to the star product representation. From the perspective of the Weyl ordering convention, Eq. (2.10) states that the Weyl ordered product of two Weyl ordered functions $f(\hat{x})$ and $g(\hat{x})$ is $(f \star g)(\hat{x})$. More physically, Eq. (2.10) represents the quantum nature of the noncommutative plane.

Although there is a complete duality between the matrix and star product representations, it is generally more convenient to work in the matrix representation in order to avoid the technical complications that are introduced by the star product. Furthermore, there is an added benefit to the matrix

formulation in that the noncommutative gauge invariance, which is discussed in Section 2.3, is manifest order by order in perturbation theory. Therefore, from this point on, we will work in the matrix representation.

2.3 Matrix Formulation of Noncommutative Gauge Theories

In Section 2.2 we introduced all of the ingredients necessary to construct noncommutative gauge theories in the matrix formulation. The correspondence given by Eq. (2.9) guarantees that an arbitrary gauge field configuration can be represented by

$$A_\mu(\hat{x}, t) = \int \frac{d^{2p}k}{(2\pi)^{2p}} e^{ik \cdot \hat{x}} \otimes \tilde{A}_\mu(k, t). \quad (2.11)$$

The tensor product in Eq. (2.11) refers to the product between the matrix structure of the exponential function of \hat{x}^i and the matrix structure of the Fourier coefficients, which we take to live in the adjoint representation of $U(N)$.

When formulating noncommutative gauge theories in the matrix representation, it is convenient to define the quantity

$$X^i(t) = \hat{x}^i \otimes \mathbb{1}_N + \theta^{ij} A_j(\hat{x}, t). \quad (2.12)$$

Eq. (2.12) implies that gauge transformations are properly realized if and only if X^i transforms in the adjoint representation of the noncommutative gauge group, which we take to be $U(N)_{\text{NC}}$

$$X^i \rightarrow U^\dagger X^i U \iff A_j \rightarrow U^\dagger A_j U + iU^\dagger \partial_j U. \quad (2.13)$$

Furthermore, space derivatives are simply given by taking the commutator

$$[X^i(t), \Phi(\hat{x}, t)] = i\theta^{ij}(D_j\Phi)(\hat{x}, t), \quad (2.14)$$

where $\Phi(\hat{x}, t)$ can be any field transforming in the adjoint representation of the gauge group and $D_j\Phi \equiv \partial_j\Phi - iA_j \star \Phi + i\Phi \star A_j$ is the gauge covariant derivative of Φ . Of course, time derivatives are defined in the standard way, and gauge covariance is achieved by introducing a gauge field $A_0(t) = A_0(\hat{x}, t)$ transforming as

$$A_0 \rightarrow U^\dagger A_0 U + iU^\dagger \dot{U} \quad (2.15)$$

under noncommutative gauge transformations.

Using the definitions of the fields X^i and A_0 , it is straight forward to show that

$$\begin{aligned} \dot{X}^i - i[A_0, X^i] &= \theta^{ij}F_{0j}(\hat{x}) \\ -i[X^i, X^j] &= \theta^{ik}\theta^{jl}(F_{kl}(\hat{x}) - \theta_{kl}^{-1}), \end{aligned} \quad (2.16)$$

where $F_{\mu\nu} \equiv \partial_\mu A_\nu - \partial_\nu A_\mu - iA_\mu \star A_\nu + iA_\nu \star A_\mu$ is the noncommutative gauge field strength. Therefore, up to total derivative terms, the Lagrangian for $2p + 1$ dimensional noncommutative Yang-Mills (NCYM)

$$L = \int d^{2p}x \text{tr}_N \left(\frac{1}{2}G^{ij}F_{0i}(x)F_{0j}(x) - \frac{1}{4}G^{ij}G^{kl}F_{ik}(x)F_{jl}(x) + \text{total deriv} \right), \quad (2.17)$$

can be recast in terms of a 0 + 1 dimensional theory of matrix fields

$$L = \text{Tr} \left(\frac{1}{2} \left(\dot{X}^i - i[A_0, X^i] \right)^2 + \frac{1}{4} [X^i, X^j] [X^i, X^j] \right), \quad (2.18)$$

where the inverse spatial metric of the field theory $G^{ij} = \theta^{ik}\theta^{kj}$. Note that for convenience, we have chosen units such that $(2\pi)^{2p}\det(\theta) = 1$.

At this point, some remarks are in order. Eq. (2.17) shows that the matrix description of NCYM given by Eq. (2.18) includes some contributions that are total space derivatives from the field theory perspective. While this is expected to be significant non-perturbatively, at least at the perturbative level, it is irrelevant because the equations of motion are unchanged. Thus, we can capture the perturbative behavior of NCYM theory by studying Eq. (2.18), which is exactly what we shall do. Another point is that this same construction can be generalized in an obvious manner to include fermions or any other matter field transforming in the adjoint representation of the gauge group. For example, the theory can be easily supersymmetrized, which we will explore in more detail in Chapters 3 and 4. Lastly, it should be noted that we can describe theories with d additional commutative spatial dimensions by simply promoting Eq. (2.17) from $0 + 1$ dimensions to $d + 1$ dimensions. We will frequently rely on this correspondence in Chapters 3 and 4 when we discuss $3 + 1$ dimensional noncommutative theories.

Before moving on to the perturbative behavior of NCYM, it is worth while discussing the noncommutative gauge invariance in more detail. From the tensor product structure of Eq. (2.12), we see that the noncommutative gauge group, which we take to be $U(N)_{\text{NC}}$, can be decomposed as $U(\infty) \otimes U(N)$, both factors generally being time-dependent. The $U(N)$ factor encodes the spatially constant part of the gauge transformation, while the $U(\infty) \equiv$

$U(1)_{\text{NC}}$ factor encodes the spatial dependence of the gauge transformation. However, due to the matrix structure of $U(\infty)$, which connects spatial points nonlocally, it is clear that noncommutative groups are a much larger group of symmetries than ordinary groups. As such, the structure imposed by the noncommutative gauge invariance will be much more rigid than that of ordinary gauge theories, and in fact all orders of the conventional perturbative expansion will contribute to gauge invariant quantities. Understanding this structure will be a central theme of this work.

Chapter 3

Perturbative Wilsonian Formalism for Noncommutative Gauge Theories

3.1 Introduction

In Chapter 2, we showed how noncommutative gauge theories are formulated in the matrix representation. We will now develop Wilsonian perturbation theory in this language in order to probe the physical effects of UV-IR mixing. We begin by rewriting Eq. (2.18) in the background field gauge, which is generally convenient in the Wilsonian approach. We then derive the propagator for the UV modes and utilize it to calculate both the leading and the next to leading order one- and two-loop corrections to the Wilsonian quantum effective action. Finally, we determine the general gauge invariant structure of perturbation theory that is valid to all loop orders in the UV regime defined by $\theta\Lambda^2 \gg 1$.

3.2 Background Field Gauge Fixing

Ultimately, we are interested in performing a Wilsonian integration of the UV modes. In order to separate the quantum effects of UV and IR states, it is convenient to work in the background field language. In this approach,

we expand the fields $A_0 = B_0 + A$ and $X^i = B^i + Y^i$, where the background fields B_0 and B^i contain the IR degrees of freedom, while the fluctuating fields A and Y^i contain the UV degrees of freedom. Of course, we can think of the background fields in the usual way, $B_0 = A_0(\hat{x})$ and $B^i = \hat{x}^i \otimes \mathbb{1}_N + \theta^{ij} A_j(\hat{x})$, using the definition given by Eq. (2.11). The fluctuating fields then have the natural interpretation as fluctuations in A_0 and A_i . The imposition of the Wilsonian cutoff is somewhat subtle, however, so that point will be deferred until Section 3.3.

In order to define the functional integral over A and Y^i , we must gauge fix the Lagrangian. This can be accomplished by adding both a gauge fixing and the corresponding ghost term to the Lagrangian

$$L_{\text{gf}} + L_{\text{gh}} = \text{Tr} \left(-\frac{1}{2} \left(-\dot{A} - i [B^i, Y^i] \right)^2 + \dot{\bar{c}} \left(\dot{c} - i[A, c] \right) + [B^i, \bar{c}] [X^i, c] \right). \quad (3.1)$$

Note that, for convenience, we have used the residual gauge symmetry of the background fields to set $B_0 = 0$, although we may restore B_0 at any time simply by gauge covariantizing the time derivatives. However, it is important to realize that no additional gauge fixing terms are required because the background fields are not to be integrated out. Upon expanding in fluctuations,

the action takes the form $L = L_0 + L_1 + L_2 + L_3 + L_4$ where

$$\begin{aligned}
L_0 &= \text{Tr} \left(\frac{1}{2} \dot{B}^{i2} + \frac{1}{4} [B^i, B^j] [B^i, B^j] \right); \\
L_2 &= \text{Tr} \left(\frac{1}{2} \dot{Y}^{j2} + \frac{1}{2} [B^i, Y^j]^2 - \frac{1}{2} \dot{A}^2 - \frac{1}{2} [B^i, A]^2 - 2i \dot{B}^i [A, Y^i] \right. \\
&\quad \left. + [B^i, B^j] [Y^i, Y^j] + \dot{c} \bar{c} + [B^i, \bar{c}] [B^i, c] \right); \\
L_3 &= \text{Tr} \left([B^i, Y^j] [Y^i, Y^j] - [B^i, A] [Y^i, A] - i \dot{Y}^i [A, Y^i] \right. \\
&\quad \left. - i \dot{c} [A, c] + [B^i, \bar{c}] [Y^i, c] \right); \\
L_4 &= \text{Tr} \left(\frac{1}{4} [Y^i, Y^j] [Y^i, Y^j] - \frac{1}{2} [A, Y^i]^2 \right). \tag{3.2}
\end{aligned}$$

Notice that we have neglected the linear term L_1 , which generically will contribute to the dynamics of the background field through tadpoles. In the language of perturbation theory, this amounts to corrections that are both higher order in the gauge coupling and higher order in derivatives of the background field. Therefore, the linear term, is suppressed if we require both that the coupling be sufficiently weak so that the loop corrections are small and that the states we integrate out be of sufficiently high momenta relative to the scale set by the background so that the higher derivative corrections are small, as well. In fact, both of these conditions will be met in our perturbative Wilsonian approach, so for the sake of simplicity, we have neglected the linear interactions in Eq. (3.2). Of course, consistency requires L_1 be included in a complete perturbative analysis, but it does not contribute to any of the quantities that we calculate in this work.

The structure of the quadratic term L_2 plays a central role in perturbation theory. We see from Eq. (3.2) that all of the fluctuating fields have similar quadratic terms up to interactions proportional to $i\dot{B}^i$ and $[B^i, B^j]$, which Eq. (2.16) implies are proportional to the background gauge field strength. As is well known, the background field dependence of the terms quadratic in the fluctuating fields can either be treated exactly or perturbatively, depending on the definition of the propagator. In our calculation, it will be most convenient to treat the field strength terms perturbatively, while absorbing the remaining background dependence into the propagator. From a physical standpoint, our treatment of L_1 and L_2 corresponds to a derivative expansion of the background field, which is valid when UV modes are integrated out. In fact, in this work, we only consider the effects of integrating out states of energy and momentum much higher than any other scale in the problem, including the noncommutativity parameter θ .

Finally, before deriving the propagator for the fluctuating fields, let us discuss the structure of expectation values in the background field language. When we compute the effects of the interaction terms in Eq. (3.2) perturbatively, we will encounter expectation values involving both background and fluctuating fields. Since the background fields are still quantum operators in the Wilsonian scheme, we cannot simply remove them from the expectation value. However, since the background and fluctuating fields contain entirely different degrees of freedom, the expectation value factorizes into a product of the expectation value of the background fields and the expectation value

of the fluctuating fields. In order to integrate out only the fluctuating fields, we evaluate the expectation value of the fluctuating fields and interpret the residual expectation value of background fields as arising from a term in the quantum effective action.

3.3 Propagator in the Matrix Representation

As discussed above, all of the fluctuating fields, $\Phi = (Y^i, A, \bar{c}, c)$ corresponding to gauge field degrees of freedom, appear similarly in quadratic terms of the form

$$\text{Tr} \left(\frac{1}{2} \dot{\Phi}^2 + \frac{1}{2} [B^i, \Phi]^2 \right). \quad (3.3)$$

In Eq. (3.3), Φ is manifestly in the adjoint representation of the noncommutative gauge group. However, it will prove convenient to express the adjoint representation as the tensor product of the fundamental and antifundamental representations. In index notation, the tensor product realization of Eq. (3.3) becomes

$$\frac{1}{2} \Phi_b^a \left(-\delta_c^b \delta_a^d \frac{d^2}{dt^2} - B_e^{ib} B_c^{ie} \delta_a^d - \delta_c^b B_e^{id} B_a^{ie} + 2B_c^{ib} B_a^{id} \right) \Phi_d^c, \quad (3.4)$$

which implies the following matrix structure

$$\frac{1}{2} \Phi^T \left(-\mathbb{1} \otimes \mathbb{1} \frac{d^2}{dt^2} - (B^i \otimes \mathbb{1} - \mathbb{1} \otimes B^i)^2 \right) \Phi. \quad (3.5)$$

In the Wilsonian scheme, we are only interested in integrating out virtual states with frequencies $\omega \gg 1/T$, T being the time scale set by the background. For these high frequency modes, the backreaction coming from

the background time dependence is a subleading effect. Therefore, the matrix propagator for virtual states with frequencies above a Wilsonian cutoff, $\Lambda \gg 1/T$, can be expressed in the following Fourier integral form

$$G(t - t') = \int_{\Lambda} \frac{d\omega}{2\pi} \frac{e^{-i\omega(t-t')}}{\omega^2 - M^2} + \dots \quad (3.6)$$

where $M^2 = (B^i \otimes \mathbb{1} - \mathbb{1} \otimes B^i)^2$ and the \dots represent subleading terms that are suppressed by factors of $(T\Lambda)^{-1} \ll 1$. In the following, we consider only the leading order term.

To relate this 0+1 dimensional matrix quantity to a $2p+1$ dimensional field theory quantity, we choose a convenient representation which is derived in Appendix B

$$\begin{aligned} & \frac{1}{\omega^2 - M^2} \\ &= \int \frac{d^{2p}k}{(2\pi)^{2p}} e^{-ik \cdot (B \otimes \mathbb{1} - \mathbb{1} \otimes B)} \int_{\theta\Lambda} d^{2p}x \frac{e^{ik \cdot (x-x')}}{\omega^2 - (x-x')^2} \\ &= \int \frac{d^{2p}k}{(2\pi)^{2p}} e^{-ik \cdot B} \otimes e^{ik \cdot B} \int_{\theta\Lambda} d^{2p}x e^{ik \cdot (x-x')} \tilde{G}(\omega, \theta^{-1}(x-x')), \end{aligned} \quad (3.7)$$

where $\tilde{G}(\omega, p) = (\omega^2 - p_i G^{ij} p_j)^{-1}$ is the field theory momentum space propagator for a massless state. As discussed in Appendix B, there is a lower cutoff applied to the integral over x such that $|x - x'| > \theta\Lambda \gg \theta/L$ where L is the length scale set by the curvature of the background. Moreover, the physical reason for imposing the cutoff on the position integral is now clear, since position apparently plays the role of momentum. Putting everything together,

the matrix propagator can be written in the following form

$$G(t - t') = \int_{\theta\Lambda} d^{2p}x \int_{\Lambda} \frac{d\omega}{2\pi} \int \frac{d^{2p}k}{(2\pi)^{2p}} e^{-i\omega(t-t') + ik \cdot (x-x')} \\ \times \tilde{G}(\omega, \theta^{-1}(x - x')) e^{-ik \cdot B(t)} \otimes e^{ik \cdot B(t)}. \quad (3.8)$$

We can now identify the various ingredients of the $0 + 1$ dimensional propagator given by Eq. (3.8) from a $2p + 1$ dimensional perspective. As suggested by the notation, (ω, k) is to be identified with the spacetime energy-momentum, and likewise, (t, x) is the corresponding spacetime coordinate. The integral over x is then understood in terms of the nonlocality of the noncommutative field theory, but perhaps more surprising is the role played by the field theory propagator, \tilde{G} . Evidently, the small- k – large- x region of the integral corresponding to low-momentum – large-distance receives contributions from *high* momentum field theory states and vice-versa. Actually, this type of behavior has a very natural interpretation in terms of the dipole degrees of freedom that we expect from the decoupling limit in which noncommutative gauge theory emerges from string theory.

In the decoupling limit, the noncommutative field quanta can be thought of as dipoles with a transverse size proportional to the center of mass momentum $(x - x')^i = \theta^{ij} p_j$. It is clear that this effect is encoded in Eq. (3.8), since the momentum argument of the field theory propagator $\tilde{G}(\omega, p)$ is $p = \theta^{-1}(x - x')$. It is also clear that, due to the Fourier integral over position, these dipole states probe a transverse momentum scale $k_i \sim 1/(x - x')^i$. Combining the two relations, we arrive at $1 \sim p_i \theta^{ij} k_j$, which is equivalent to the stationarity

of the Moyal phase factors that appear in the star product formulation [7]. In essence, this relation means that integrating out high momentum states can lead to low momentum effects – a symptom of UV-IR mixing. Thus, it seems that Eq. (3.8) naturally describes the dipole degrees of freedom that appear in noncommutative gauge theories.

However, it is important to realize that the representation of the propagator given by Eq. (3.8) is only valid for dipoles of high energy and momentum. More precisely, if the background changes on time and length scales T and L , respectively, we can only integrate over frequencies $\omega \gg 1/T$ and momenta $p = \theta^{-1}(x - x') \gg 1/L$; otherwise, the time derivatives and commutators involving the background field that were dropped in the derivation of Eq. (3.8) are no longer negligible. Therefore, the cutoff Λ is chosen such that $\Lambda \gg 1/T$ and $1/L$, in which case the higher order commutator and time derivative corrections are suppressed by factors of $(L\Lambda)^{-1}$ and $(T\Lambda)^{-1} \ll 1$. Moreover, since the cutoff is chosen relative to the scale of the background, Λ is naturally interpreted in the Wilsonian sense.

The matrix structure of the $0 + 1$ dimensional propagator, which is contained entirely in the tensor product of operators of the form $\exp(ik \cdot B)$, also has an important field theory interpretation. As derived in Appendix C, we can identify

$$e^{ik \cdot B(t)} = e^{ik \cdot \hat{x} \otimes 1_N + ik \cdot \theta \cdot A(\hat{x}, t)} \longleftrightarrow P_\star e^{i \int_0^1 d\sigma k \cdot \theta \cdot A(x + \sigma \theta \cdot k, t)} \star e^{ik \cdot x}, \quad (3.9)$$

where P_\star denotes path ordering of the exponential using the star product. This

object transforms in the adjoint under gauge transformation, and in particular, the trace is gauge invariant

$$\mathrm{Tr} \left(e^{ik \cdot B(t)} \right) \longleftrightarrow \int d^{2p}x e^{ik \cdot x} \mathrm{tr}_N \left(P_{\star} e^{i \int_0^1 d\sigma k \cdot \theta \cdot A(x + \sigma \theta \cdot k, t)} \right). \quad (3.10)$$

We immediately recognize this object as the Fourier transform of an open Wilson line . In fact, this structure was essentially guaranteed by the noncommutative gauge invariance [21].

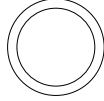
When we use the matrix propagator for perturbative calculations of the quantum effective action, we will frequently encounter the Fourier transform of Eq. (3.10). Following [15], we define the operator

$$\rho(x, t) = \int \frac{d^{2p}k}{(2\pi)^{2p}} e^{ik \cdot x} \mathrm{Tr} \left(e^{-ik \cdot B(t)} \right). \quad (3.11)$$

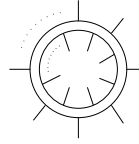
Although $\rho(x)$ is generally a spatially nonlocal field theory operator, for $\theta \cdot k$ sufficiently small such that Eq. (3.8) is valid, it is approximately local on length scales given by the background configuration, as can be easily seen from Eqs. (3.10) and (3.11). In fact, all gauge invariant Wilson line operators, which differ only by extra operator insertions, will share this property. For example, an insertion of an arbitrary operator \mathcal{O} into the end of the Wilson line gives

$$\rho_{\mathcal{O}}(x, t) = \int \frac{d^{2p}k}{(2\pi)^{2p}} e^{ik \cdot x} \mathrm{Tr} \left(\mathcal{O}(t) e^{-ik \cdot B(t)} \right). \quad (3.12)$$

The interpretation of the matrix propagator in terms of dipole degrees of freedom is made more concrete in Sections 3.4 and 3.5 by calculating the



(a) Single matrix diagram is manifestly gauge invariant and implicitly contains all leading background dependence.



(b) Gauge invariance achieved by summing over all background insertions on both the outer and inner boundaries.

Figure 3.1: One-loop contributions in the matrix versus the star product approach.

leading and next to leading order one- and two-loop corrections to the Wilsonian quantum effective action. We will find that integrating out UV virtual states gives rise to long-distance interaction terms that are naturally interpreted in the dipole context discussed above.

3.4 One-loop Corrections to the Effective Action

We begin the computation of the quantum effective action at one-loop, where the advantage of the matrix formulation becomes immediately clear. The leading one-loop contribution is manifestly gauge invariant and can be expressed in a single diagram drawn in 't Hooft double line notation as shown in Fig. 3.1(a). This is to be contrasted with the field theory star product approach in which an infinite number of diagrams of the form shown in Fig. 3.1(b) must be summed up in order to achieve gauge invariance [12, 13, 14].

Using the matrix representation of the propagator given by Eq. (3.8), the evaluation of the matrix diagram is simple. The contraction of matrix

indices, as indicated by the double line diagram, gives a double trace contribution proportional to

$$\begin{aligned}
& (N_B - N_F) \int dt dt' \delta(t - t') \text{Tr} \log G(t - t') \\
&= (N_B - N_F) \int dt d^{2p} x_1 d^{2p} x_2 \rho(x_1, t) \rho(x_2, t) \int \frac{d\omega}{2\pi} \log \tilde{G}(\omega, \theta^{-1} x_{12}),
\end{aligned} \tag{3.13}$$

where $x_{12} \equiv x_1 - x_2$, and N_B and N_F are the numbers of on-shell bosonic and fermionic polarization states, respectively. Note that, although we have discussed only the gauge degrees of freedom explicitly, fermions and other matter fields will generally contribute quantities of the same form as the pure gauge calculation, but they will differ in the constant of proportionality, as in Eq. (3.13) above. Furthermore, the integrals are always assumed to be cutoff as previously discussed, even though the cutoff will often be suppressed.

Now let us understand the structure of Eq. (3.13) a bit more in terms of the conventional field theory diagrams that are illustrated in Fig. 3.1(b). First of all, we choose to expand $\rho(x) = \text{tr}_N(\mathbb{1}) + \Delta(x)$. The significance of $\Delta(x)$ is that it contains only fluctuations of the background field around the vacuum state. In particular, $\Delta(x)$ vanishes for trivial configurations gauge equivalent to $A_i(x) = 0$, which can be seen from Eqs. (3.10) and (3.11). Therefore, the field theory interpretation of $\Delta(x)$ is that it represents the gauge invariant contribution from the insertions of the background gauge field into a boundary of the loop. On the other hand, the constant term of $\rho(x)$ is gauge field independent, and therefore, must descend from field theory diagrams with no

background insertions into the corresponding outer or inner boundary.

For example, we can conclude that the Δ^0 term involves no insertions on either the outer or the inner boundary, and therefore, comes from field theory vacuum diagrams. Using the same reasoning, we find that the Δ^1 terms involve background insertions on only one boundary, and therefore, are due to non-vacuum planar field theory diagrams. Finally, the Δ^2 term involves insertions on both the outer and the inner boundary, and therefore, arises from nonplanar field theory diagrams. Thus, the single matrix diagram in Fig. 3.1(a) contains contributions from both planar and nonplanar field theory diagrams.

However, Eq. (3.13) only reproduces the leading order terms of the expansion in external momenta, as can be verified by a direct field theory calculation [15]. The reason is that in deriving Eq. (3.8), the matrix formulation naturally leads to an expansion in commutators and time derivatives. The subleading terms, as we have seen, are suppressed by factors of $(L\Lambda)^{-1}$, $1/L$ being the scale of the external momenta and Λ the scale of the Wilsonian cutoff. This must correspond to the expansion in external momenta of the field theory propagators in the loop diagrams, since the expansion parameter is the same. On the other hand, the external momentum dependence of the Moyal phase factors is determined exactly by noncommutative gauge invariance. In terms of the structure that we discussed in Section 3.3, the expansion in the external momenta of the propagators manifests itself as higher dimensional operator insertions into the end of the Wilson lines as in Eq. (3.12), while the Wilson lines themselves are the manifestation of both the additional

propagators and the Moyal phase factors associated to the external insertions. Thus, as alluded to earlier, the physical nature of our approximation is that of a standard derivative expansion of the background. In fact, order by order, the matrix approach reproduces the momentum expansion of the field theory propagators if higher order commutators and time derivatives are retained.

Back to the evaluation of Eq. (3.13), the vacuum diagrams, corresponding to the Δ^0 term, are divergent. It is easy to see that they are proportional to

$$\begin{aligned} & (N_B - N_F)N^2V \int dt \frac{d\omega}{2\pi} d^{2p}x_{12} \log \tilde{G}(\omega, \theta^{-1}x_{12}) \\ &= (N_B - N_F)N^2V \int dt \frac{d\omega d^{2p}p}{2\pi(2\pi)^{2p}} \log \tilde{G}(\omega, p). \end{aligned} \quad (3.14)$$

In fact, this is nothing but the usual one-loop UV vacuum divergence that is familiar from ordinary field theories. The leading one-loop divergent contribution from other non-vacuum planar diagrams, which corresponds to the Δ^1 term, vanishes because $\int d^{2p}x \Delta(x) = 0$, as can be seen from Eq. (3.11). Thus, in the case of planar field theory diagrams, the leading one-loop correction reduces to known results.

On the other hand, the nonplanar diagrams represented by the Δ^2 interaction

$$(N_B - N_F) \int dt d^{2p}x_1 d^{2p}x_2 \Delta(x_1, t) \Delta(x_2, t) \int \frac{d\omega}{2\pi} \log \tilde{G}(\omega, \theta^{-1}x_{12}), \quad (3.15)$$

demonstrates an entirely new effect. This term illustrates how UV dipoles can mediate long-distance interactions. When the virtual dipoles in the loop

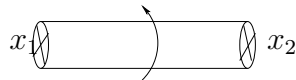


Figure 3.2: High momentum virtual dipoles grow long in the transverse direction and mediate instantaneous interactions between distant background fluctuations at x_1 and x_2 .

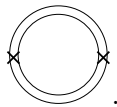
have high momentum, Fig. 3.1(a) “stretches out” into a long cylinder that joins distant points x_1 and x_2 . Each boundary of the cylinder contributes a trace which yields a gauge invariant Wilson line operator corresponding to low momentum background insertions into the field theory diagrams. This process is depicted in Fig. 3.2. *Thus, we can interpret the double lines of the matrix diagram as literally representing the end points of the virtual dipole quanta as they propagate around the loops.*

In fact, by performing the integration over frequency, we can calculate the interaction strength between $\Delta(x_1)$ and $\Delta(x_2)$

$$\int \frac{d\omega}{2\pi} \log \tilde{G}(\omega, \theta^{-1}x_{12}) \sim |x_1 - x_2| + \text{constant}. \quad (3.16)$$

Thus, in the presence of this term, the theory is strongly interacting at long distances. This fact has been recognized in [15], and it was shown that these strong long-distance interactions are due to the leading IR pole singularities that appear in nonsupersymmetric noncommutative theories. The appearance of nonanalytic behavior in external momenta has also been discussed in the star product formulation in [4, 5, 6, 7, 8, 9, 10, 11, 12, 13, 14]. However, if the theory is supersymmetric, then $N_B = N_F$ and the leading order one-loop interaction given by Eq. (3.13) vanishes.

We must now consider the next to leading order one-loop contribution, which has also been discussed from the star product perspective in [13]. As alluded to earlier, the precise result requires that we keep the next to leading order commutators and time derivatives that were dropped in the derivation of the propagator, as well as extra insertions of the background field strength coming from terms in L_2 that were also excluded from the propagator. However, power counting as well as symmetry arguments imply that the next to leading order one-loop contribution will be of the same order as Fig. 3.1(a) with two extra insertions of the field strength



This contribution alone suffices to demonstrate the qualitative features of the next to leading order one-loop behavior. It has the added virtue that the calculation can be done with the leading order propagator Eq. (3.8) because the field strength insertions are already higher order. A straight forward calculation outlined in Appendix D leads to a term in the action of the form

$$\int dt d^{2p}x_1 d^{2p}x_2 \left[c_1 \rho_{FF}(x_1, t) \rho(x_2, t) + c_2 \rho_F(x_1, t) \rho_F(x_2, t) \right] \times \int \frac{d\omega}{2\pi} \tilde{G}(\omega, \theta^{-1}x_{12}) \tilde{G}(\omega, \theta^{-1}x_{21}), \quad (3.17)$$

where the subscript F denotes an insertion of the field strength into the end of the Wilson line.

At this point, there are several comments to be made. First of all, it is clear that Eq. (3.17) describes the instantaneous interaction between two

points x_1 and x_2 , which is consistent with the long dipole picture depicted in Fig. 3.2. Moreover, all one-loop matrix diagrams, which differ only by higher dimensional operator insertions, must have a similar double trace structure, and hence, give rise to two-body interactions. Secondly, note that the appearance of the propagator \tilde{G} is again consistent with our intuition from field theory. In fact in Section 3.5, we will see that this property is a direct result of the gauge invariant structure of perturbative corrections. Lastly, we can identify a term in Eq. (3.17) that leads to one-loop renormalization of the gauge coupling.

The one-loop renormalization comes from a UV divergence in the planar sector, corresponding to the constant part of ρ in the first term of Eq. (3.17).

The integral over position then factorizes into

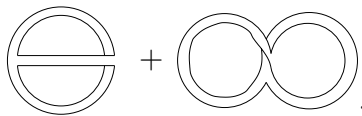
$$\begin{aligned}
& N \int dt d^{2p}x_1 \rho_{FF}(x_1, t) \int \frac{d\omega}{2\pi} d^{2p}x_{12} \tilde{G}(\omega, \theta^{-1}x_{12})^2 \\
&= N \int dt \text{Tr} \left(\dot{B}^{i2} + [B^i, B^j]^2 \right) \int \frac{d\omega d^{2p}p}{2\pi(2\pi)^{2p}} \tilde{G}(\omega, p)^2. \quad (3.18)
\end{aligned}$$

This quantity is easily recognized as the familiar one-loop contribution to the renormalization of the gauge coupling. Although a systematic treatment of renormalization will have to wait for Chapter 4, we can already see from Eqs. (3.14) and (3.18) that UV dipoles in planar diagrams can lead to UV divergences and conventional renormalization of the parameters in the theory. Of course, we shall assume a negative beta function so that our perturbative Wilsonian approach is valid.

3.5 Higher Loop Corrections to the Effective Action

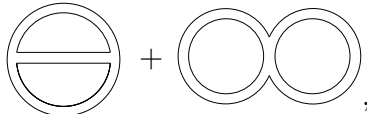
In the analysis of one-loop corrections to the quantum effective action, we found that matrix diagrams naturally lead to multi-trace operators, which had the physical interpretation of instantaneous multi-body interactions mediated by long dipoles. We will now extend our analysis to include higher order loop effects. Ultimately, we will determine the general gauge invariant structure of perturbation theory which will be exploited in the Chapter 4 to compute the divergence structure of noncommutative gauge theory.

One of the entirely new features of higher order loops is the appearance of nonplanar matrix diagrams. For example, in the case of the leading order two-loop diagrams, we have nonplanar cubic and quartic diagrams



As discussed in Appendix E, nonplanar matrix diagrams correspond to field theory diagrams in which the loops are linked in a nonplanar fashion. However, nonplanar diagrams seem to correspond to physics not described by the dipole degrees of freedom that form the basis for our perturbative analysis. Therefore, the validity of our analysis requires that we suppress the contribution of nonplanar matrix diagrams to the Wilsonian integration. It was shown in Appendix E that when $\theta\Lambda^2 \gg 1$, nonplanar matrix diagrams are negligible compared to planar ones due to exponential suppression from Moyal phase factors. *Thus, in the UV domain of Wilsonian integration given by $\theta\Lambda^2 \gg 1$, the contribution from nonplanar matrix diagrams is negligible.*

Continuing with the leading order two-loop planar matrix diagrams



we find triple trace contributions indicated by the double line notation. As calculated in Appendix E, the quartic diagram gives an interaction term in the effective action proportional to

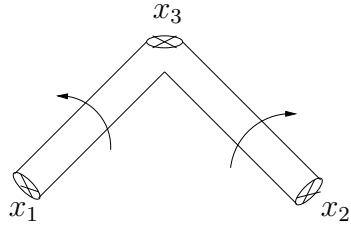
$$\int dt d^{2p}x_1 d^{2p}x_2 d^{2p}x_3 \rho(x_1, t) \rho(x_2, t) \rho(x_3, t) \times \int \frac{d\omega_1}{2\pi} \frac{d\omega_2}{2\pi} \tilde{G}(\omega_1, \theta^{-1}x_{13}) \tilde{G}(\omega_2, \theta^{-1}x_{23}), \quad (3.19)$$

and the cubic diagram gives a term proportional to

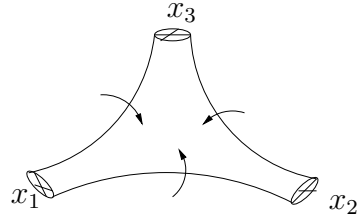
$$\int dt d^{2p}x_1 d^{2p}x_2 d^{2p}x_3 \rho(x_1, t) \rho(x_2, t) \rho(x_3, t) \times \int \frac{d\omega_1}{2\pi} \frac{d\omega_2}{2\pi} (\omega_1 \omega_2 - x_{12} \cdot x_{23}) \tilde{G}(\omega_1, \theta^{-1}x_{12}) \times \tilde{G}(\omega_2, \theta^{-1}x_{23}) \tilde{G}(\omega_1 + \omega_2, \theta^{-1}x_{31}). \quad (3.20)$$

Indeed, as expected based on our intuition, Eqs. (3.19) and (3.20) describe long-distance interactions that arise from high momentum dipoles growing large in spatial extent and “stretching out” the matrix diagrams, as depicted in Fig. 3.3. Furthermore, these expressions bear a close resemblance to what is expected from ordinary field theory, and in fact, the general structure of perturbative corrections is starting to emerge.

To each boundary of the double line diagram we should associate a point in space and a trace which yields a gauge invariant Wilson line. The position dependence of the interaction strength between the Wilson lines follows



(a) An illustration of the contribution from the first order treatment of quartic interaction terms given by (3.19).



(b) An illustration of the contribution from the second order treatment of cubic interaction terms given by (3.20).

Figure 3.3: Long distance three-body interactions corresponding to high momentum dipoles propagating in two-loop diagrams.

from an integral over frequencies with the integrand being given by a particular function of both the dipole frequencies and momenta as defined by the separation between the space points associated to the boundaries of the double line diagram. In fact, the particular function of dipole frequencies and momenta corresponds precisely to the structure of momentum space field theory propagators that appear in the analogous process in ordinary field theory.

The subleading terms in the derivative expansion must have a similar trace structure but Wilson lines modified to include higher derivative operator insertions as in Eq. (3.17). Naturally, the subleading terms will include a different function of dipole frequencies and momenta that reflects the extra propagators that are required by the operator insertions. Since powers of momentum are equivalent to powers of separation for dipole degrees of freedom, the inclusion of more powers of momentum in the denominator naively leads to faster falloff with distance, which is expected from subleading terms in a

derivative expansion. However, quantum corrections coming from higher loop orders are generally strong, as we will discuss in Chapter 4. To further reinforce these ideas, we have included an outline of the calculation of the next to leading order two-loop planar matrix diagrams in Appendix F.

Let us now exploit our understanding of the general gauge invariant structure to obtain a result that holds to all orders of perturbation theory. First of all, it is clear that at L -loop order the leading interactions will involve $L + 1$ Wilson lines with no operator insertions, such as Eq. (3.13) in the case $L = 1$ and both Eq. (3.19) and Eq. (3.20) in the case $L = 2$. The crucial observation is that since the vacuum diagrams are contained in interactions of this form, as shown explicitly by Eq. (3.14) in the one-loop case, the leading order terms must vanish entirely if the vacuum diagrams vanish. For example, this result implies that for supersymmetric noncommutative theories the leading interactions must cancel at each order in perturbation theory. This statement is a generalization to all loop orders of the cancellation that we have already seen in the case of the leading one-loop interactions given by Eq. (3.13). It reflects the fact that supersymmetric theories are softer in the UV, and hence, the IR behavior that is generated by UV-IR mixing is not as strong. The relation between the amount of supersymmetry and the cancellation of non-analytic terms in external momenta has been discussed in [10, 11] from the field theory perspective.

Actually, we can extend this line of reasoning much farther. In order to do so, let us take some time to discuss the proportionality constants that

we have thus far ignored. Consider the content of the matrix diagrams from a field theory point of view. First of all, the double line matrix diagrams themselves only contain information pertaining to the contraction of gauge indices, which encodes the planarity and nonplanarity of both the external operator insertions and the internal propagators. Thus, the double line diagrams contain purely topological information, not specific to any particular gauge theory – ordinary or noncommutative. In terms of the framework that we have discussed up to this point, this topological information only fixes the ratio of coefficients between terms with a similar propagator structure but different Wilson line structure. For example, in Eq. (3.17) the ratio between c_1 and c_2 is fixed by purely topological considerations. It also follows that the coefficients of nonplanar matrix diagrams are fixed relative to the coefficients of the corresponding planar diagrams (Note that factors of N result from the traces that are included in the Wilson lines and loops and are not contained in the coefficients as we have defined them). The essential point is that topological quantities, such as the ratio between coefficients of diagrams involving a similar propagator structure, are independent of most characteristics specific to the theory in question such as the field content, coupling constants, and whether the theory is noncommutative or not. Topological quantities can only depend on properties that determine how double lines can be “glued” together to form diagrams.

Nonetheless, the coefficients of matrix diagrams involving a similar propagator structure all share a common normalization factor that depends

on the number and type of modes that propagate around the loops. Thus, the overall normalization factor does depend on characteristics specific to a particular theory, such as the field content and the coupling constants. However, the noncommutativity of the theory enters only through the Moyal phase factors inside the momentum integrals of nonplanar field theory diagrams; noncommutativity does not affect the coefficient multiplying the integral. After all, the combinatorics associated with the contraction of fields is the same in both cases. *Thus, the coefficients of double line matrix diagrams in a given noncommutative gauge theory are equal to the corresponding coefficients of double line diagrams in the ordinary counterpart gauge theory.*

It follows immediately that the nonrenormalization theorems enjoyed by ordinary supersymmetric theories generalize to noncommutative supersymmetric theories. For example, we already know that even minimal supersymmetry leads to the vanishing of the leading order matrix diagrams – both planar and nonplanar – to all orders in perturbation theory. However, we can now make some much stronger statements. For example, by imposing 3 + 1 dimensional $\mathcal{N} = 2$ supersymmetry, we can eliminate all corrections to the gauge coupling beyond one loop. In this case, the next to leading order one-loop correction given by Eq. (3.17) is not constrained, but supersymmetry does impose restrictions at the two-loop level. As discussed in Appendix F, b_6 contains the two-loop correction to the beta function, which must vanish. Since b_7 and b_8 are also proportional to b_6 by the arguments above, Eq. (F.3) must vanish entirely for 3+1 dimensional $\mathcal{N} = 2$ noncommutative Super Yang-Mills

(NCSYM) theory. In the case of $3 + 1$ dimensional $\mathcal{N} = 4$ NCSYM theory, none of the next to leading order interactions are allowed at all.

In summary, we have shown how dipole degrees of freedom naturally emerge from a manifestly gauge invariant perturbative treatment of noncommutative gauge theories in the UV regime defined by $\theta\Lambda^2 \gg 1$. The essential result of this Chapter, however, was the determination of the gauge invariant form of perturbative corrections to the Wilsonian quantum effective action. In particular, we were able to relate the proportionality constants of double line matrix diagrams that appear in noncommutative gauge theories to the corresponding constants in ordinary gauge theories, with which we are familiar and many results are known. In Chapter 4, we shall exploit this isomorphism to its fullest extent in order to make powerful statements about the divergence structure of noncommutative gauge theories.

Chapter 4

Application of the Perturbative Wilsonian Formalism to the Divergence Structure

4.1 Introduction

We will now systematically analyze the divergence structure of the perturbative corrections to the Wilsonian quantum effective action. In the process of integrating out UV modes, in addition to UV divergences, we encounter new divergences having dual UV and IR interpretations. Using the structural results discussed in Chapter 3, we are able to show that, to all orders in perturbation theory, the pure UV divergences can be cancelled by standard renormalization of the parameters in the theory, but the UV-IR divergences can only be cancelled by adding terms of an entirely new form to the action. We then discuss self-consistency conditions on noncommutative gauge theories and nonrenormalization theorems that prevent the appearance of UV-IR divergences. We also briefly discuss IR divergences that arise from the naive perturbative treatment of the quantum effective action.

4.2 Divergences and UV-IR Mixing

In Section 3.4, we calculated the one-loop divergences. They were shown to be of the standard UV form and merely contribute to the renormalization of the vacuum energy and the gauge coupling. However, we shall now show that the effect of UV-IR mixing on the divergence structure enters at the two-loop level and qualitatively changes the types of divergences that can appear. There are pure UV divergences, dual UV-IR divergences, and pure IR divergences.

Let us start by discussing the IR divergences. These divergences do not arise directly from the Wilsonian integration of the UV modes, but rather, arise from the integration of IR modes in the context of a naive perturbative treatment of the quantum effective action. The most primitive two-loop example comes from the interactions given by Eq. (3.13). To see this, it is convenient to Fourier transform to momentum space, in which case we get

$$\int dt \frac{d\omega d^{2p}p}{(2\pi)(2\pi)^{2p}} \frac{d^{2p}k}{(2\pi)^{2p}} e^{ip \cdot \theta \cdot k} \tilde{\rho}(k, t) \tilde{\rho}(-k, t) \log \tilde{G}(\omega, p). \quad (4.1)$$

We now perturbatively expand the Wilson lines

$$\tilde{\rho}(k, t) = N(2\pi)^{2p} \delta^{2p}(k) + ik \cdot \theta \cdot \text{tr}_N \tilde{A}(k, t) + \dots, \quad (4.2)$$

and contract the terms linear in the gauge field. The result is proportional to

$$NV \int \frac{d\omega d^{2p}p}{(2\pi)(2\pi)^{2p}} \frac{d\omega' d^{2p}k}{(2\pi)(2\pi)^{2p}} k^2 e^{ip \cdot \theta \cdot k} \tilde{G}(\omega', k) \log \tilde{G}(\omega, p), \quad (4.3)$$

where the UV loop momentum $p > \Lambda$ and the IR loop momentum $k < \Lambda$. To recast Eq. (4.3) into a more familiar form, we must rewrite

$$k^2 e^{ip \cdot \theta \cdot k} = -ik \cdot \theta^{-1} \cdot \partial_p (e^{ip \cdot \theta \cdot k}), \quad (4.4)$$

and integrate by parts to obtain

$$NV \int \frac{d\omega d^{2p} p}{(2\pi)(2\pi)^{2p}} \frac{d\omega' d^{2p} k}{(2\pi)(2\pi)^{2p}} ik \cdot \theta \cdot p e^{ip \cdot \theta \cdot k} \tilde{G}(\omega', k) \tilde{G}(\omega, p). \quad (4.5)$$

Again, we manipulate Eq. (4.5) by rewriting

$$-ik \cdot \theta \cdot p e^{ip \cdot \theta \cdot k} = \partial_\sigma e^{i\sigma p \cdot \theta \cdot k} \Big|_{\sigma=1}. \quad (4.6)$$

After re-scaling the frequencies and momenta, it is easy to see that Eq. (4.5) reduces to the familiar form of the IR divergent two-loop nonplanar vacuum diagram whose contribution is given by Eq. (E.5). Therefore, this well-known IR divergence that is ubiquitous in noncommutative quantum field theories is actually contained in the contribution to the effective action of the one-loop planar matrix diagram. In fact, it is clear that in our Wilsonian framework, IR divergent nonplanar diagrams always appear from the contraction of external insertions on distinct boundaries of UV divergent planar matrix diagrams. The reason is that, due to Moyal phase factors, nonplanar loop diagrams contribute only when some loop momenta are in the UV, while others are in the IR. Thus, the existence of IR divergences in nonplanar loop diagrams is directly related to the existence of UV divergences in planar matrix diagrams.

It follows that the IR divergences can be cancelled by any mechanism that cancels the UV divergent planar diagrams, such as minimal supersymmetry in $2 + 1$ dimensions or maximal supersymmetry in $3 + 1$ dimensions.

Although, it should be noted that it is possible that the IR divergences do not need to be cancelled. Perhaps IR divergences can be dealt with by reorganizing the perturbative expansion in some manner. For example, the resummation of the leading nonanalytic momentum dependence into the propagator has been proposed in [7], but this technique only works for theories containing a matter content such that the leading nonanalytic term has the proper sign for the summation not to lead to an instability [13, 15]. Other authors have studied the IR behavior of noncommutative gauge theories in the context of the star product formulation of Wilsonian integration [10]. However, it could well be that a deeper structural understanding of the theory is required in order to resolve the problem of IR divergences. In fact, it may turn out that the weakly coupled dipoles that are valid for $\theta\Lambda^2 \gg 1$ may not be the correct degrees of freedom when $\theta\Lambda^2 \lesssim 1$ and nonplanar matrix diagrams become important. In any event, we expect that the gauge invariant Wilson loop structure associated with nonplanar diagrams will play a prominent role in resolving this issue.

A further discussion of the systematic treatment of IR divergences is beyond the scope of this work. Instead, we seek to understand the divergences that emerge directly from the Wilsonian integration of UV modes. Let us consider the leading order two-loop diagrams, which can be combined into the form of Eq. (3.19). It is now straight forward to isolate the divergent terms by using the splitting scheme $\rho(x) = \text{tr}_N(\mathbb{1}) + \Delta(x)$ that was discussed in

Section 3.4. The constant term in either $\rho(x_1)$ or $\rho(x_2)$ gives

$$\int dt d^{2p}x_1 d^{2p}x_3 \rho(x_1, t) \rho(x_3, t) \int \frac{d\omega_1}{2\pi} \tilde{G}(\omega_1, \theta^{-1}x_{13}) \int \frac{d\omega_2 d^{2p}p_2}{2\pi(2\pi)^{2p}} \tilde{G}(\omega_2, p_2). \quad (4.7)$$

Apparently, Eq. (4.7) involves the one-loop UV divergent contribution to the mass term of the field theory propagator \tilde{G} appearing in Eq. (3.13), which is a familiar type of correction from our experience with ordinary quantum field theories. Of course, gauge invariance prevents these type of corrections to the gauge field propagator, and more generally, supersymmetry can be employed to cancel them in all cases. Nonetheless, the meaning of Eq. (4.7) is that it represents a one-loop correction to the one-loop interaction given by Eq. (3.13); it does not contain an inherently two-loop correction to the theory. Furthermore, the diagrammatical interpretation of Eq. (4.7) is that it contains the contribution from a one-loop planar subdiagram, which necessarily involves a loop integration that is decoupled from the Moyal phase factors. Since Moyal phase factors are the source of UV-IR mixing, this means that divergences in planar subdiagrams always have a purely UV interpretation.

The other distinct group of terms in the contribution of the leading order two-loop diagrams comes from the constant term of $\rho(x_3)$

$$\int dt d^{2p}x_1 d^{2p}x_2 \rho(x_1, t) \rho(x_2, t) \int \frac{d\omega_1}{2\pi} \frac{d\omega_2 d^{2p}p_3}{2\pi(2\pi)^{2p}} \tilde{G}(\omega_{21}, p_3 - \theta^{-1}x_{12}) \tilde{G}(\omega_2, p_3). \quad (4.8)$$

First, we consider the UV divergent contributions from the planar subdiagrams contained in Eq. (4.8). The leading order contribution from planar

non-vacuum diagrams vanishes, as usual, because $\int d^{2p}x \Delta(x) = 0$. However, the vacuum diagrams, which are contained in the constant terms of $\rho(x_1)$ and $\rho(x_2)$, give the two-loop correction to the renormalization of the vacuum energy. This is to be contrasted with the vacuum diagrams contained in Eq. (4.7), which give the mass correction to the propagators in the one-loop vacuum diagrams. In fact, this example shows how the structure added by the background insertions removes all ambiguities associated with overlapping divergences.

The nonplanar diagrams contained in Eq. (4.8), corresponding to the Δ^2 term, evidently represent a two-loop quantum correction to the interaction strength of Eq. (3.15). The growth in $|x_1 - x_2|$ of this correction is given by

$$\int \frac{d\omega_1}{2\pi} \frac{d\omega_2 d^{2p}p_3}{2\pi(2\pi)^{2p}} \tilde{G}(\omega_{21}, p_3 - \theta^{-1}x_{12}) \tilde{G}(\omega_2, p_3), \quad (4.9)$$

which is clearly divergent for $p \geq 1$. In order to understand the meaning of divergent loop diagrams with nonplanar external insertions, such as those contained in Eq. (4.8), it is instructive to look at the interaction in momentum space

$$\int dt \frac{d^{2p}k}{(2\pi)^{2p}} \tilde{\Delta}(k, t) \tilde{\Delta}(-k, t) \frac{d\omega_1 d^{2p}q}{2\pi(2\pi)^{2p}} \frac{d\omega_2 d^{2p}p}{2\pi(2\pi)^{2p}} e^{ik \cdot \theta \cdot q} \tilde{G}(\omega_{21}, p - q) \tilde{G}(\omega_2, p), \quad (4.10)$$

because the role of the Moyal phase factors is clarified. We can first perform the integrals over ω_2 and p by introducing a Schwinger parameter and an UV cutoff M , as in [7]. Then the integral over ω_1 and q is regular, and we are left

with a quantity proportional to

$$\begin{aligned} & \int dt \frac{d^{2p}k}{(2\pi)^{2p}} \frac{\tilde{\Delta}(k, t)\tilde{\Delta}(-k, t)}{(k^2 + 1/M^2)^{2p-1}} \\ &= \int dt d^{2p}x_1 d^{2p}x_2 \Delta(x_1, t)\Delta(x_2, t) \int \frac{d^{2p}k}{(2\pi)^{2p}} \frac{e^{ik \cdot (x_1 - x_2)}}{(k^2 + 1/M^2)^{2p-1}}. \end{aligned} \quad (4.11)$$

Now the $M \rightarrow \infty$ limit results in a divergence in the IR region of integration in a Fourier transform instead of the UV region of integration in a loop integral, and $1/M$ plays the role of an IR cutoff. The transform back into position space yields a leading order interaction strength of the form $|x_1 - x_2|^{2p-2} \log(|x_1 - x_2|^2/M^2)$, which could also be determined directly from Eq. (4.9).

Apparently, divergences in loop diagrams with nonplanar external insertions have a dual UV-IR interpretation. In the case of Eq. (4.10), the origin of this duality can be traced to the Moyal phase factor $\exp(ik \cdot \theta \cdot q)$, which represents the nonplanarity of the background insertions and gives rise to UV-IR mixing. In particular, the UV loop integrals over virtual states, labelled by momenta p and q , produce nonanalytic dependence on the background momentum k that becomes important in the IR. In other words, the divergence comes from integrating over UV states, but on the other hand, it can be recast into the form of an IR singular Fourier transform.

Actually, this type of UV-IR mixing has a simple interpretation in terms of dipole degrees of freedom. The separation between the endpoints of the dipoles is the dual variable to the external momenta k . Therefore, the IR singular Fourier transform gives rise to corrections to interaction strengths which grow strong with large separation. However, since powers of separation

are equivalent to powers of dipole momentum, these strong corrections can also be thought of as arising from UV divergences in the theory. Thus, the dipole intuition that emerges from the matrix formulation seems to shed new light on the proposal of [5] concerning the dual interpretation of divergences in nonplanar diagrams, although our treatment of UV-IR divergences will be much different than theirs.

Although we have surveyed only the contribution from the leading order two-loop diagrams explicitly, it is straight forward to perform a similar analysis on the next to leading order two-loop diagrams that were calculated in Appendix F. It is easy to see that the next to leading order divergence structure is qualitatively similar. In fact, the divergence structure of all the subleading terms in the derivative expansion will be qualitatively similar to the examples that we have discussed explicitly, although in $3 + 1$ dimensions or fewer, power counting implies that there are no divergences of any kind beyond the next to leading order. However, it remains to be seen what the effect of higher order loop corrections will mean for the quantum-mechanical self-consistency of noncommutative gauge theories.

4.3 Treatment of UV and UV-IR Divergences

In Section 4.2, we gained a two-loop introduction to the types of divergences that appear in noncommutative theories. We found pure UV divergences, dual UV-IR divergences, and pure IR divergences. While the proper treatment of the IR divergences lies beyond the scope of this work, we will

be able to understand the structure of both the UV and UV-IR divergences. Ultimately this divergence structure follows from the gauge invariant form of perturbative corrections that we determined in Section 3.5 and the diagrammatical combinatorics, which we shall discuss below.

As we have seen explicitly at the one- and two-loop levels, the divergent loop integrations appearing in planar subdiagrams have a pure UV interpretation and are structurally consistent with the renormalization of parameters such as the vacuum energy, mass, and gauge coupling. In fact, it is easy to see that the UV divergence structure is consistent with parameter renormalization to all loop orders. Moreover, there are no ambiguities posed by overlapping divergences due to the structure added by the external background insertions, which are automatically included in this formalism. However, it is not yet clear whether the combinatorics of the planar subdiagrams is consistent with renormalizability to all orders in perturbation theory.

Actually, it turns out that the diagrammatical combinatorics of non-commutative theories is isomorphic to that of the ordinary counterpart theories. To see this, it is helpful to consider the contribution from matrix diagrams – at any order in the derivative expansion, planar, or nonplanar – in energy-momentum space. For example, Eq. (3.13) becomes

$$\int \frac{d^{2p+1}p}{(2\pi)^{2p+1}} \frac{d^{2p+1}k}{(2\pi)^{2p+1}} e^{ip \cdot \theta \cdot k} \tilde{\rho}(k) \tilde{\rho}(-k) \log \tilde{G}(p), \quad (4.12)$$

where $\tilde{\rho}(k) = N(2\pi)^{2p+1} \delta^{2p+1}(k) + \tilde{\Delta}(k)$. Clearly, the contribution from any matrix diagram can be written this way by Fourier transforming the Wilson

lines and loops and interpreting the separation between the endpoints of the virtual dipoles as a momentum variable instead of a separation variable. The point is that, other than the Moyal phase factor and the particular form of $\tilde{\Delta}(k)$, Eq. (4.12) it is identical to what is expected from ordinary gauge theory. Furthermore, this statement is true for any matrix diagram whatsoever – the interpretation is that $\tilde{\Delta}(k)$ encodes the gauge invariant contribution of background insertions of net momentum k into the boundary of the diagram; while the delta function term reduces to the contribution from diagrams with no insertions on the corresponding boundary.

The crucial observation is that the diagrammatical combinatorics, which follows from expanding $\tilde{\rho}$ as above, is completely independent of the Moyal phase factors and the particular form of $\tilde{\Delta}$. Therefore, the diagrammatical combinatorics of a particular noncommutative gauge theory is absolutely identical to that of the ordinary counterpart, which we shall assume to be renormalizable. Since we know that renormalizability can be understood in the context of the $1/N$ expansion, which separates planar and nonplanar contributions, it follows immediately that the UV divergences that occur in planar subdiagrams of noncommutative theories can be cancelled by parameter renormalization to all orders in perturbation theory. It does not matter that nonplanar diagrams are no longer UV divergent when the theory is noncommutative; it only matters that the combinatorics are such that the divergences in the planar subdiagrams can be cancelled by parameter renormalization. *Thus, renormalizability of UV divergences is a property inherited by noncommutative*

gauge theories from their ordinary counterparts.

It follows that a necessary condition for the removal of the UV cut-off in a given noncommutative gauge theory is that the ordinary counterpart gauge theory be renormalizable. Therefore, we can only consider (spatially) noncommutative theories living in either $2 + 1$ or $3 + 1$ dimensions, if we demand that the theory be self-consistent quantum-mechanically. Of course, this was to be expected based on our intuition from ordinary quantum field theories. However generally, there are still UV-IR divergent terms which appear as corrections to the strength of lower order long-distance interactions, which are described by purely nonplanar diagrams. In fact, we can reduce the divergence structure down to purely nonplanar form by extracting all of the UV divergences from planar subdiagrams via renormalization. Then, any remaining divergence must come from purely nonplanar diagrams, and therefore, must be of the UV-IR type.

Actually, as shown explicitly at the two-loop order in Section 4.2, the existence of UV-IR divergences is directly related to the existence of higher loop order corrections to the renormalization of the theory. The reason is that the UV-IR divergences that are new at a given loop order can only come from the group of terms containing the UV divergent planar diagrams that contribute a higher loop order correction to renormalization, because all other planar subdiagrams simply amount to lower order loop corrections. Put another way, UV-IR divergent nonplanar diagrams correspond precisely to the contribution from otherwise planar subdiagrams that would give higher order

corrections to renormalization were it not for extra nonplanar external insertions. Therefore, UV-IR divergences will generally appear in noncommutative theories that allow renormalization beyond the one-loop order.

Actually, there is an accidental exception to this rule which is due to g^2 having mass dimension one in $2 + 1$ dimensions. To see this, we need only consider the leading order terms in the derivative expansion, since only they allow divergences in this case. Furthermore, it is easy to see that the two-body Δ^2 interactions

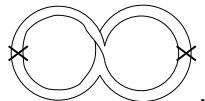
$$\int dt d^2x_1 d^2x_2 \Delta(x_1, t) \Delta(x_2, t) \left(|x_1 - x_2| + \text{higher loop corrections} \right), \quad (4.13)$$

are the only dangerous terms. Based on dimensional analysis, the two-loop term in Eq. (4.13) is of the form $g^2 \log(|x_1 - x_2|^2/M^2)$, which is also consistent with Eq. (4.9). However, in this case, the actual logarithmic divergence does not contribute due to $\int dx \Delta(x) = 0$. Moreover, three-loop and higher corrections are finite since the degree of divergence is lower at each order. Therefore, in $2 + 1$ dimensions, UV-IR divergences do not appear. Of course, this same argument does not work in $3 + 1$ dimensions because there are new logarithmic divergences at each order in perturbation theory. In the particular case of Eq. (4.13), the higher loop corrections in $3 + 1$ dimensions are of the form of powers of the dimensionless quantity $g^2 \log(|x_1 - x_2|^2/M^2)$ multiplying the one-loop term, which goes as $|x_1 - x_2|^2 \log(|x_1 - x_2|^2/M^2)$.

Thus, UV-IR divergences occur in noncommutative gauge theories of dimension $3 + 1$ or higher if and only if renormalization beyond one loop is

allowed. Furthermore, these UV-IR divergences cannot be cancelled by parameter renormalization, because structurally they contribute entirely new terms to the action. For this reason, quantum-mechanical self-consistency requires that the appearance of UV-IR divergences, and hence renormalization beyond one loop, is not allowed. Of course, nonrenormalization properties of this type require supersymmetry, which is simply a statement that softer UV behavior is necessary to control the proliferation of UV-IR divergences arising from UV-IR mixing. In fact, it is interesting that in $3 + 1$ dimensions minimal $\mathcal{N} = 1$ supersymmetry is not sufficient; at least $\mathcal{N} = 2$ is required to protect against renormalization beyond one-loop order, and hence, UV-IR divergences.

One must keep in mind, however, that the consistent removal of the UV cutoff does not necessarily imply the theory is well behaved in the IR. In fact, our analysis in Section 4.2 implies that if UV divergences are allowed at all, IR divergences will appear in the naive perturbative treatment of the Wilsonian quantum effective action. For example, $3 + 1$ dimensional $\mathcal{N} = 2$ NCSYM, which allows only a one-loop renormalization of the gauge coupling, contains IR divergences in the next to leading order nonplanar diagrams such as



In $2 + 1$ dimensions, IR divergences generally appear in the leading order two-loop nonplanar diagram. In fact, the only way to eliminate these IR problems

completely in the context of the conventional perturbative expansion discussed in this work, is to demand at least minimal supersymmetry in $2+1$ dimensions and maximal supersymmetry in $3+1$ dimensions. As discussed in Section 4.2, it remains an interesting and important open problem as to whether or not this is necessary for consistency.

On another note, it is tempting to extend our results to noncommutative theories other than gauge theories. After all, the intuition that we have gained appears to be quite generic and most likely applies to any noncommutative theory. For example, it seems unlikely that $3+1$ dimensional noncommutative scalar theory is self-consistent quantum-mechanically, when nonsupersymmetric $3+1$ dimensional gauge theories are not. It even seems reasonable that self-consistency could break down in $\mathcal{N} = 1$ and $\mathcal{N} = 2$ supersymmetric noncommutative theories that do not include gauge degrees of freedom, in light of the fact that any extra hypermultiplets of matter that are added to $\mathcal{N} = 2$ NCSYM theory must form particular representations which do not allow all orders of wave function renormalization.

Nonetheless, arguments have been put forward for the quantum consistency of many noncommutative theories that are excluded by our analysis [6]. Although, these works have involved different approaches which have encoded UV-IR mixing in one way or another, none have employed a manifestly dipole construction such as the matrix formulation. Since the dipole behavior of the elementary quanta is the fundamental origin of UV-IR mixing in noncommutative theories, it seems that the physical interpretation that naturally

emerges from the matrix approach is the most reliable. We believe that this is a tremendous advantage when discussing the divergence structure, because traditionally, the proper treatment of divergences has resulted from a sound physical interpretation for their meaning. Of course, the physical content of noncommutative theories is independent of the language used to discuss them; we are simply suggesting that the physics is more clear in the matrix representation.

Ultimately, the essential difference between our work and [6] is the interpretation and treatment of the dual UV-IR divergences that occur in noncommutative quantum theories. Other authors have employed independent UV and IR cutoffs in their analysis. They have found that the UV divergences can be renormalized and the UV cutoff removed while the UV-IR and IR divergences are cutoff independently in the IR (Actually, they do not distinguish between UV-IR and IR divergences). Of course, this result is not inconsistent with our analysis, but at some point the IR cutoff must be removed in which case the UV-IR divergences reappear. In other words, by independently cutting off the IR, they inadvertently hide the UV-IR divergences which actually come directly from the UV region of integration, and therefore, must be dealt with before the UV cutoff is removed. In fact, independent UV and IR cutoffs are not even consistent with UV-IR mixing because UV and IR degrees of freedom cannot be separately removed from the theory due to their mutual nondecoupling. Thus, the results of [6] may not be entirely reliable.

Before closing, let us make a few comments concerning the scope of our

results from the perspective of string theory. Our analysis has been limited to noncommutative gauge theories, and given these dipole degrees of freedom, we have shown that both a sufficiently high degree of supersymmetry and low spacetime dimensionality is necessary to ensure the quantum mechanical consistency of the theory. However, this result does not imply that other degrees of freedom cannot be added to the theory to give a consistent completion. For example, [22] shows that there is an UV completion of some higher dimensional NCSYM theories in the form of noncommutative open string theories, in which the closed string sector has decoupled but there are still stringy modes from the open string sector that remain. Yet another distinct possibility is that, in the case of theories with a lesser degree of supersymmetry, there could be some closed string modes that survive the decoupling limit and render the theory consistent [23]. The point is that any theory that emerges from an exact decoupling limit of string theory must be consistent; our results only imply that the decoupled theory can conceivably be a noncommutative gauge theory in only very special cases.

Chapter 5

Discussion and Outlook

In this work, we have developed the perturbative Wilsonian treatment of noncommutative gauge theories in the matrix formulation. These methods proved to be instrumental in understanding the effects of UV-IR mixing. In particular, we were able to make significant progress in two main respects.

First, we were able to directly observe the fundamental dipole structure of the elementary quanta. These dipoles had the property that they extended proportionately in the transverse direction to their center of mass momentum, which is expected from a string theory analysis of the decoupling limit that leads to noncommutative gauge theory. Furthermore, we found that the dipole character emerged naturally from the matrix representation and was manifestly embodied by the propagator. When UV states were integrated out, the perturbative corrections to the Wilsonian quantum effective action included nonlocal interaction terms that were structurally consistent with the dipole behavior of the intermediate virtual quanta. In the end, UV-IR mixing could be understood as originating from the dipole nature of the theory: UV dipoles grow long in spatial extent and mediate instantaneous long-distance interactions that are relevant in the IR.

Secondly, we found that UV-IR mixing has a profound effect on the divergence structure of the theory. In the process of integrating out UV modes, we encountered divergences having pure UV and dual UV-IR interpretations. The pure UV divergences were shown to contribute to the renormalization of parameters in the theory when the dimensionality does not exceed $3 + 1$. On the other hand, the dual UV-IR divergences, which were shown to appear in dimensionality greater than $2 + 1$, could not be cancelled by parameter renormalization. Instead, we had to invoke a minimum of $\mathcal{N} = 2$ supersymmetry in $3 + 1$ dimensions. Furthermore, it was shown that a naive perturbative analysis of the Wilsonian quantum effective action results in IR divergences in any dimensionality. The general treatment of these IR divergences required a structural understanding beyond the scope of this work; although, it was shown that minimal supersymmetry in $2 + 1$ dimensions and maximal supersymmetry in $3 + 1$ dimensions were sufficient to eliminate all IR divergences from the theory.

The main tool that we employed in our analysis was noncommutative gauge invariance. The understanding of the gauge invariant structure of perturbative corrections to the quantum effective action enabled us to extend our analysis to all orders of perturbation theory, both in terms of what nonlocal interactions and divergences are allowed to appear. Moreover, the gauge invariant structure, particularly in regards to the connection between Wilson loops and nonplanar diagrams, is likely to play a central role in understanding the IR regime of Wilsonian integration in noncommutative gauge theories. In

particular, it is not even known how to describe the IR degrees of freedom that are valid when $\theta\Lambda^2 \lesssim 1$; our analysis, based on dipole degrees of freedom, is only reliable in the UV regime given by $\theta\Lambda^2 \gg 1$. Nonetheless, we expect that the IR degrees of freedom receive large contributions from the UV, and are likely described by manifestly nonlocal objects such as Wilson lines and loops. Understanding the IR regime of Wilsonian integration is perhaps the most interesting and important problem that remains unsolved in the subject of noncommutative gauge theories.

However, as discussed in the introduction, there are more fundamental reasons to understand the role of noncommutative gauge invariance. While the preliminary steps in analyzing the behavior of noncommutative gauge theories have not obviously shed much light on either duality or holography, we have been able to gain some intuition for how nonlocal gauge invariance (not to be confused with invariance under global symmetries) can give rise to spatially extended degrees of freedom that exhibit UV-IR mixing. Both of these ingredients are necessary in any holographic theory, so it is possible that some hint of progress has been made in this direction. Duality, on the other hand, does not seem to be illuminated at all by our study of noncommutative gauge symmetry, although it is possible that some sort of duality emerges between the degrees of freedom in the UV and those in the IR [24].

Nevertheless, this work is significant in the sense that it contributes to the development of noncommutative gauge theories themselves. Fundamental physics aside, noncommutative gauge theories are interesting in their own

right, mainly because they exhibit manifest spatial nonlocality and UV-IR nondecoupling. Both of these properties have posed major challenges to the understanding of noncommutative quantum field theories. This work has shed a great deal of light on how to formulate and interpret the physics of such theories, as well as open the door for future studies in the area. We look forward to finding out where this line of research will ultimately lead.

Appendices

Appendix A

Orthogonality and Completeness Relations for the Fourier Matrix Basis

In this Appendix, we will derive the orthogonality and completeness relations for the Fourier matrix basis discussed in Section 2.2. Our approach will be to explicitly derive the results in the case of two noncommutative dimensions, the generalization to arbitrary dimensionality being obvious.

It is convenient to rewrite the matrix coordinates, which satisfy $[\hat{x}_1, \hat{x}_2] = i\theta\mathbb{1}$, in terms of operators satisfying $[a, a^\dagger] = \mathbb{1}$

$$\hat{x}_1 = \sqrt{\frac{\theta}{2}}(a^\dagger + a) \quad \hat{x}_2 = i\sqrt{\frac{\theta}{2}}(a^\dagger - a). \quad (\text{A.1})$$

In this case, the Fourier basis matrices become

$$\begin{aligned} & \exp\left(i\sqrt{\frac{\theta}{2}}(k_1 + ik_2)a^\dagger + i\sqrt{\frac{\theta}{2}}(k_1 - ik_2)a\right) \\ &= \exp\left(-\frac{\theta}{4}(k_1^2 + k_2^2)\right) \exp\left(i\sqrt{\frac{\theta}{2}}(k_1 + ik_2)a^\dagger\right) \exp\left(i\sqrt{\frac{\theta}{2}}(k_1 - ik_2)a\right). \end{aligned} \quad (\text{A.2})$$

We can now compute the matrix element $\langle z_1 | e^{ik \cdot \hat{x}} | z_2 \rangle$, where

$$|z\rangle = \exp\left(-\frac{|z|^2}{2}\right) \sum_n \frac{(za^\dagger)^n}{n!} |0\rangle \quad (\text{A.3})$$

is the normalized eigenstate of a with eigenvalue z . Using Eqs. (A.2) and (A.3) we get

$$\langle z_1 | e^{ik \cdot \hat{x}} | z_2 \rangle = e^{-\frac{\theta}{4}k^2 + i\sqrt{\frac{\theta}{2}}(k_1 + ik_2)\bar{z}_1 + i\sqrt{\frac{\theta}{2}}(k_1 - ik_2)z_2} \langle z_1 | z_2 \rangle \quad (\text{A.4})$$

$$\langle z_1 | z_2 \rangle = e^{-\frac{1}{2}|z_1|^2 - \frac{1}{2}|z_2|^2 + \bar{z}_1 z_2}. \quad (\text{A.5})$$

By performing the integrals in radial coordinates defined by $z = re^{i\phi}$, it is easy to show that the trace can be expressed as

$$\text{Tr}(e^{ik \cdot \hat{x}}) = \int \frac{dz d\bar{z}}{2\pi i} \langle z | e^{ik \cdot \hat{x}} | z \rangle. \quad (\text{A.6})$$

Using Eq. (A.4) and rewriting $z = \frac{1}{\sqrt{2\theta}}(x_1 + ix_2)$, we find Eq. (A.6) is equal to

$$\int \frac{d^2x}{2\pi\theta} e^{ik \cdot x - \frac{\theta}{4}k^2} = \frac{(2\pi)^2 \delta^2(k)}{2\pi\theta}, \quad (\text{A.7})$$

which can be easily generalized to the $2p$ -dimensional case by taking p tensor products of independent two-planes. In the end, we arrive at Eq. (2.4). Again using Eq. (A.4), it is straight forward to show that

$$\int \frac{d^2k}{(2\pi)^2} \langle z_1 | e^{ik \cdot \hat{x}} | z_2 \rangle \langle z_3 | e^{-ik \cdot \hat{x}} | z_4 \rangle = \frac{\langle z_1 | z_4 \rangle \langle z_3 | z_2 \rangle}{2\pi\theta} \quad (\text{A.8})$$

by performing the gaussian k integrals. The fact that Eq. (A.8) holds for arbitrary z_1, z_2, z_3 , and z_4 implies Eq. (2.5) after generalizing to $2p$ dimensions.

Appendix B

Propagator in the Fourier Matrix Basis

In order to clarify the field theory interpretation of the matrix propagator, we seek a representation of the form

$$\frac{1}{\omega^2 - M^2} = \int \frac{d^{2p}k}{(2\pi)^{2p}} e^{-ik \cdot (B \otimes 1 - 1 \otimes B)} \tilde{c}(k). \quad (\text{B.1})$$

The Fourier coefficients, $\tilde{c}(k)$, can be constrained by acting with $\omega^2 - M^2$

$$\begin{aligned} 1 &= \int \frac{d^{2p}k}{(2\pi)^{2p}} (\omega^2 - M^2) e^{-ik \cdot (B \otimes 1 - 1 \otimes B)} \tilde{c}(k) \\ &= \int \frac{d^{2p}k}{(2\pi)^{2p}} (\omega^2 + \partial_k^2) e^{-ik \cdot (B \otimes 1 - 1 \otimes B)} \tilde{c}(k) + \dots, \end{aligned} \quad (\text{B.2})$$

where the \dots represent commutator terms that are necessary to resolve the ordering of the noncommuting matrices, $B^i \otimes \mathbb{1} - \mathbb{1} \otimes B^i$. It is easy to see that the commutator corrections are negligible if

$$B^i \gg [k \cdot B, B^i], [k \cdot B, [k \cdot B, B^i]], \dots \quad (\text{B.3})$$

Using Eqs. (2.12) and (2.14) along with the expression for B^i , we see that $[k \cdot B, \] = k \cdot \theta \cdot D$ where D_i is the gauge covariant derivative. Therefore the commutators are small if $\theta \cdot k \ll L$, L being the length scale set by the curvature of the background.

Assuming that the commutators are negligible, we may keep only the leading term in above equation. Then, upon an integration by parts, the condition on the fourier coefficients becomes

$$(\omega^2 + \partial_k^2) \tilde{c}(k) = (2\pi)^{2p} \delta^{2p}(k). \quad (\text{B.4})$$

From this equation, we arrive at the integral expression

$$\tilde{c}(k) = \int d^{2p}x \frac{e^{ik \cdot (x-x')}}{\omega^2 - (x-x')^2}. \quad (\text{B.5})$$

Note that the consistency condition $\theta \cdot k \ll L$ can be implemented by imposing $|x - x'| \gg \theta/L$. As we will see in Section 3.3, there is a physical reason to impose the cutoff on the x integral rather than the k integral. Therefore, we will apply a cutoff of the form $|x - x'| > \theta\Lambda \gg \theta/L$. Putting everything together, up to commutator terms that are suppressed by factors of $(L\Lambda)^{-1} \ll 1$, we obtain the desired representation given by Eq. (3.7).

Appendix C

Equivalence Between the Fourier Basis Matrices and Wilson Lines

In this Appendix, we shall verify that the Fourier basis matrices $e^{ik \cdot \hat{x}}$ correspond to Wilson lines, which was first obtained in [21]. We begin by rewriting

$$e^{ik \cdot B} = \left(e^{\frac{i}{N} k \cdot B} \right)^N. \quad (\text{C.1})$$

Substituting in the expression for the background field $B^i = \hat{x}^i + \theta^{ij} A_j(\hat{x})$, we obtain

$$\left(e^{\frac{i}{N} k \cdot \hat{x} + \frac{i}{N} k \cdot \theta \cdot A(\hat{x})} \right)^N = \left(e^{\frac{i}{N} k \cdot \hat{x}} e^{\frac{i}{N} k \cdot \theta \cdot A(\hat{x}) + \dots} \right)^N, \quad (\text{C.2})$$

where the \dots represent higher derivatives of the gauge field given by powers of $\frac{1}{N} k \cdot \theta \cdot \partial$ acting on $k \cdot \theta \cdot A(\hat{x})$. However, for arbitrary $A(\hat{x})$ satisfying the physical boundary condition that the field configuration vanish at infinity, we may choose N large enough to suppress the higher derivative terms. In particular, we have

$$e^{ik \cdot B} = \lim_{N \rightarrow \infty} \left(e^{\frac{i}{N} k \cdot \hat{x}} e^{\frac{i}{N} k \cdot \theta \cdot A(\hat{x})} \right)^N. \quad (\text{C.3})$$

We can now expand the product as follows

$$\prod_{n=1}^N \left(e^{i \frac{n}{N} k \cdot \hat{x}} e^{\frac{i}{N} k \cdot \theta \cdot A(\hat{x})} e^{-i \frac{n}{N} k \cdot \hat{x}} \right) e^{ik \cdot \hat{x}} = \prod_{n=1}^N \left(e^{\frac{i}{N} k \cdot \theta \cdot A(\hat{x} + \frac{n}{N} \theta \cdot k)} \right) e^{ik \cdot \hat{x}}. \quad (\text{C.4})$$

Again, we use the fact that physical field configurations must vanish at infinity, so that in the $N \rightarrow \infty$ limit we may keep only up to order $1/N$ in each exponential factor

$$\lim_{N \rightarrow \infty} \prod_{n=1}^N \left(e^{\frac{i}{N} k \cdot \theta \cdot A(\hat{x} + \frac{n}{N} \theta \cdot k)} \right) = \lim_{N \rightarrow \infty} \prod_{n=1}^N \left(1 + \frac{i}{N} k \cdot \theta \cdot A \left(\hat{x} + \frac{n}{N} \theta \cdot k \right) \right). \quad (\text{C.5})$$

It is now convenient to introduce the discrete path ordered exponential

$$\begin{aligned} P \exp_N \left(\sum_{n=1}^N \frac{i}{N} k \cdot \theta \cdot A \left(\hat{x} + \frac{n}{N} \theta \cdot k \right) \right) &\equiv \\ 1 + \sum_{J=1}^N \sum_{n_1 < \dots < n_J} &\underbrace{\frac{i}{N} k \cdot \theta \cdot A \left(\hat{x} + \frac{n_1}{N} \theta \cdot k \right) \cdots \frac{i}{N} k \cdot \theta \cdot A \left(\hat{x} + \frac{n_J}{N} \theta \cdot k \right)}_{J \text{ factors}}, \end{aligned} \quad (\text{C.6})$$

which is defined as the finite sum of $N + 1$ terms, as in Eq. (C.6) above, and approaches the standard path ordered exponential in the $N \rightarrow \infty$ limit. By using Eqs. (C.3), (C.4), (C.5), and (C.6) and taking the continuum limit, we have

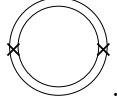
$$e^{ik \cdot B} = P e^{i \int d\sigma k \cdot \theta \cdot A(\hat{x} + \sigma \theta \cdot k)} e^{ik \cdot \hat{x}}. \quad (\text{C.7})$$

Finally, using the correspondence defined by Eqs. (2.9) and (2.10) we arrive at Eq. (3.9).

Appendix D

Next to Leading Order One-Loop Diagram

As discussed in Section 3.4, the structure of the next to leading order one-loop contribution can be obtained by computing



A straight forward second order perturbative treatment of the interaction term in L_2 that is proportional to $[B^i, B^j]$ yields a quantity of the form

$$\begin{aligned}
 & \int dt_1 d^{2p}x_1 dt_2 d^{2p}x_2 \int \frac{d\omega_1 d^{2p}k_1}{2\pi(2\pi)^{2p}} \frac{d\omega_2 d^{2p}k_2}{2\pi(2\pi)^{2p}} e^{-i\omega_1(t_1-t_2)+ik_1 \cdot x_1} e^{-i\omega_2(t_2-t_1)+ik_2 \cdot x_2} \\
 & \quad \times \tilde{G}(\omega_1, \theta^{-1}x_1) \tilde{G}(\omega_2, \theta^{-1}x_2) \left[c_1 \text{Tr} \left([B^i, B^j](t_1) e^{ik_1 \cdot B(t_1)} [B^i, B^j](t_2) \right. \right. \\
 & \quad \times e^{-ik_2 \cdot B(t_2)} \left. \left. \text{Tr} \left(e^{-ik_1 \cdot B(t_1)} e^{ik_2 \cdot B(t_2)} \right) + c_2 \text{Tr} \left([B^i, B^j](t_1) e^{ik_1 \cdot B(t_1)} \right. \right. \right. \\
 & \quad \times e^{-ik_2 \cdot B(t_2)} \left. \left. \left. \text{Tr} \left([B^i, B^j](t_2) e^{-ik_1 \cdot B(t_1)} e^{ik_2 \cdot B(t_2)} \right) \right] \right). \quad (\text{D.1})
 \end{aligned}$$

Since we only integrate out virtual states with high energy and momentum, time derivatives of the background as well as higher commutator terms are

further suppressed. Therefore, to lowest order, we obtain

$$\begin{aligned}
& \int dt d^{2p}x_1 d^{2p}x_2 \int \frac{d\omega}{2\pi} \frac{d^{2p}k_1}{(2\pi)^{2p}} \frac{d^{2p}k_2}{(2\pi)^{2p}} e^{ik_1 \cdot x_1} e^{ik_2 \cdot x_2} \tilde{G}(\omega, \theta^{-1}x_1) \tilde{G}(\omega, \theta^{-1}x_2) \\
& \times \left[c_1 \text{Tr} \left([B^i, B^j](t) [B^i, B^j](t) e^{i(k_1 - k_2) \cdot B(t)} \right) \text{Tr} \left(e^{-i(k_1 - k_2) \cdot B(t)} \right) \right. \\
& \quad \left. + c_2 \text{Tr} \left([B^i, B^j](t) e^{i(k_1 - k_2) \cdot B(t)} \right) \text{Tr} \left([B^i, B^j](t) e^{-i(k_1 - k_2) \cdot B(t)} \right) \right].
\end{aligned} \tag{D.2}$$

Note that the global $SO(2p, 1)$ symmetry of Eq. (2.18) requires that the time derivatives appear in the combination given by $\dot{B}^{i2} + [B^i, B^j]^2$. Upon Fourier transforming to position space, we are finally left with Eq. (3.17).

Appendix E

Leading Order Two-Loop Diagrams

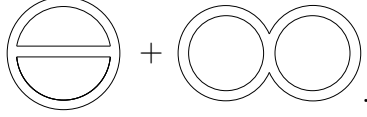
The leading two-loop diagrams come from the first order perturbative treatment of the quartic interaction terms in L_4 and the second order perturbative treatment of the cubic interaction terms in L_3 . A straight forward evaluation of the relevant matrix elements gives quantities proportional to

$$\begin{aligned} & \int dt d^{2p}x_1 d^{2p}x_2 \int \frac{d\omega_1 d^{2p}k_1}{2\pi(2\pi)^{2p}} \frac{d\omega_2 d^{2p}k_2}{2\pi(2\pi)^{2p}} e^{ik_1 \cdot x_1} e^{ik_2 \cdot x_2} \tilde{G}(\omega_1, \theta^{-1}x_1) \tilde{G}(\omega_2, \theta^{-1}x_2) \\ & \quad \times \left[\text{Tr}\left(e^{ik_1 \cdot B(t)}\right) \text{Tr}\left(e^{-ik_2 \cdot B(t)}\right) \text{Tr}\left(e^{-ik_1 \cdot B(t)} e^{ik_2 \cdot B(t)}\right) \right. \\ & \quad \quad \left. - \text{Tr}\left(e^{ik_1 \cdot B(t)} e^{ik_2 \cdot B(t)} e^{-ik_1 \cdot B(t)} e^{-ik_2 \cdot B(t)}\right) \right], \end{aligned} \quad (\text{E.1})$$

in the case of the quartic interactions and

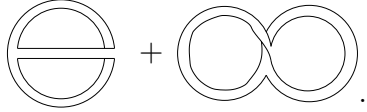
$$\begin{aligned} & \int dt_1 dt_2 d^{2p}x_1 d^{2p}x_2 d^{2p}x_3 \int \frac{d\omega_1 d^{2p}k_1}{2\pi(2\pi)^{2p}} \frac{d\omega_2 d^{2p}k_2}{2\pi(2\pi)^{2p}} \frac{d\omega_3 d^{2p}k_3}{2\pi(2\pi)^{2p}} e^{-i\omega_1(t_1-t_2)+ik_1 \cdot x_1} \\ & \quad \times e^{-i\omega_2(t_1-t_2)+ik_2 \cdot x_2} e^{-i\omega_3(t_1-t_2)+ik_3 \cdot x_3} \tilde{G}(\omega_1, \theta^{-1}x_1) \tilde{G}(\omega_2, \theta^{-1}x_2) \\ & \quad \times \tilde{G}(\omega_3, \theta^{-1}x_3) \left(\omega_1 \omega_2 + \frac{\partial}{\partial k_2} \cdot \frac{\partial}{\partial k_3} \right) \left[\text{Tr}\left(e^{ik_1 \cdot B(t_1)} e^{ik_2 \cdot B(t_1)}\right) \text{Tr}\left(e^{-ik_1 \cdot B(t_1)} \right. \right. \\ & \quad \times e^{ik_3 \cdot B(t_2)} \left. \left. \text{Tr}\left(e^{-ik_2 \cdot B(t_1)} e^{-ik_3 \cdot B(t_2)}\right) - \text{Tr}\left(e^{ik_1 \cdot B(t_1)} e^{-ik_3 \cdot B(t_2)} e^{-ik_2 \cdot B(t_1)} \right. \right. \right. \\ & \quad \left. \left. \times e^{-ik_1 \cdot B(t_1)} e^{ik_3 \cdot B(t_2)} e^{ik_2 \cdot B(t_1)} \right) \right], \end{aligned} \quad (\text{E.2})$$

in the case of the cubic interactions. The structure of the triple trace terms is by now familiar, and they correspond to the planar matrix diagrams



Using by now familiar techniques, we neglect the higher order commutators and time derivatives in order to obtain Eq. (3.19) from Eq. (E.1) and Eq. (3.20) from Eq. (E.2), after a Fourier transformation to position space.

The single trace terms, on the other hand, are qualitatively new, and they correspond to the nonplanar matrix diagrams



Let us take some time to understand the structure of these contributions. In the case of the single trace term from Eq. (E.1), using Eq. (3.9), we can simplify the trace as follows

$$\begin{aligned} & \text{Tr} \left(e^{ik_1 \cdot B} e^{ik_2 \cdot B} e^{-ik_1 \cdot B} e^{-ik_2 \cdot B} \right) \\ &= e^{ik_1 \cdot \theta \cdot k_2} \int dx_3 \text{tr}_N \left(P_{\star} e^{i \oint_C d\gamma \cdot A(x_3 + \gamma)} \right), \end{aligned} \quad (\text{E.3})$$

where the contour $C = C(k_1, k_2)$ is the parallelogram defined by the vectors $\theta \cdot k_1$ and $\theta \cdot k_2$. Using similar techniques, it is easy to see that the single trace term in Eq. (E.2) reduces to a Wilson loop defined by a hexagonal contour. Thus, in the case of nonplanar matrix diagrams, the gauge invariant contribution of background gauge field insertions can form Wilson loops, in addition to Wilson lines.

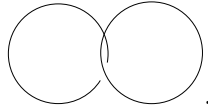
We can shed further light on the meaning of nonplanar matrix diagrams by considering the vacuum diagram associated with the single trace term of Eq. (E.1), which is obtained by setting $A_i = 0$. This leaves a quantity proportional to

$$NV \int dt d^{2p}x_1 d^{2p}x_2 \int \frac{d\omega_1 d^{2p}k_1}{2\pi(2\pi)^{2p}} \frac{d\omega_2 d^{2p}k_2}{2\pi(2\pi)^{2p}} e^{ik_1 \cdot x_1} e^{ik_2 \cdot x_2} \times e^{ik_1 \cdot \theta \cdot k_2} \tilde{G}(\omega_1, \theta^{-1}x_1) \tilde{G}(\omega_2, \theta^{-1}x_2). \quad (\text{E.4})$$

Upon performing the k integrals, we are left with

$$NV \int dt \frac{d\omega_1 d^{2p}p_1}{2\pi(2\pi)^{2p}} \frac{d\omega_2 d^{2p}p_2}{2\pi(2\pi)^{2p}} e^{ip_1 \cdot \theta \cdot p_2} \tilde{G}(\omega_1, p_1) \tilde{G}(\omega_2, p_2), \quad (\text{E.5})$$

where we have changed variables of integration to $p = \theta^{-1}x$. Eq. (E.5) is easily recognized as the contribution to the effective action from the two-loop nonplanar field theory vacuum diagram



Thus, nonplanar matrix diagrams correspond to field theory diagrams with the loops linked in a nonplanar fashion.

However, when $\theta\Lambda^2 \gg 1$, nonplanar loop diagrams do not contribute to the Wilsonian integration. To see this, consider the integration over ω, p in Eq. (E.5)

$$\begin{aligned} & \int_{\Lambda} \frac{d\omega_1 d^{2p}p_1}{2\pi(2\pi)^{2p}} \frac{d\omega_2 d^{2p}p_2}{2\pi(2\pi)^{2p}} e^{ip_1 \cdot \theta \cdot p_2} \tilde{G}(\omega_1, p_1) \tilde{G}(\omega_2, p_2) \\ \sim & \int_{\Lambda} \frac{d^{2p}p_1}{|\theta p_1|} \frac{d^{2p}p_2}{|\theta p_2|} e^{ip_1 \cdot \theta \cdot p_2} \sim \Lambda^{4p-2} e^{-\theta\Lambda^2}, \end{aligned} \quad (\text{E.6})$$

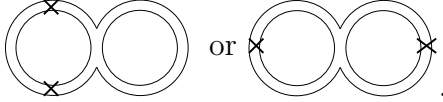
where the final integration can be performed with Schwinger parameters in the stationary phase approximation. Thus, in the UV domain of Wilsonian integration, the contribution from nonplanar matrix diagrams is exponentially suppressed due to Moyal phase factors and, therefore, negligible compared to planar matrix diagrams. In fact, we will restrict our analysis to the $\theta\Lambda^2 \gg 1$ regime in order to avoid nonplanarity. The reason is that, according to the intuition that we have so far developed, each trace is associated with a point in space, and therefore, the reduction in the number of traces that occurs in nonplanar matrix diagrams is most naturally interpreted as some kind of short-distance effect. Since the intuitive picture of UV dipoles propagating in loops that we discussed in Section 3.4 is not compatible with the notion short-distance quantum corrections, we regard the nonplanar contributions that emerge when $\theta\Lambda^2 \lesssim 1$ as indicating the presence of different degrees of freedom in the IR – possibly Wilson loop in nature.

Nonetheless, nonplanar matrix diagrams can, in principle, be treated in the context of the background derivative expansion. As usual, one thinks of the k variables as small, and therefore, expands the Wilson loop. This provides the insertion of higher dimensional operators into the trace as well as higher powers of k , which are equivalent to more powers of momentum in the denominator by means of integration by parts. However, one cannot expand the $\exp(k_1 \cdot \theta \cdot k_2)$ factor, since it leads to the Moyal phase factor that ultimately suppresses the contribution.

Appendix F

Next to Leading Order Two-Loop Diagrams

As in the next to leading order one-loop calculation, to get the precise result we must retain higher order commutators and time derivatives that were dropped in the derivation of the matrix propagator Eq. (3.8) as well as the field strength terms in L_2 that were also excluded from the the propagator. However, after already developing some intuition for the structure of terms that can appear, a lengthy calculation is not necessary. We simply need to keep track of all the distinct possibilities in which the field strength insertions can appear in the diagrams. For example, in the case of the quartic diagram, both insertions can go into one loop or each loop can get a single insertion



Of course, each insertion requires an extra field theory propagator to appear in the corresponding loop, and for each loop, there are two boundaries in which the insertion can go. Therefore, the first diagram corresponding to both insertions going into the same loop contributes two terms

$$\int dt d^{2p}x_1 d^{2p}x_2 d^{2p}x_3 \int d\omega_1 d\omega_2 \tilde{G}(\omega_1, \theta^{-1}x_{13})^3 \tilde{G}(\omega_2, \theta^{-1}x_{23}) \times \left[b_1 \rho_{FF}(x_1, t) \rho(x_2, t) \rho(x_3, t) + b_2 \rho_F(x_1, t) \rho(x_2, t) \rho_F(x_3, t) \right], \text{(F.1)}$$

while the second diagram corresponding to one insertion going into each loop contributes three terms

$$\begin{aligned} & \int dt d^{2p}x_1 d^{2p}x_2 d^{2p}x_3 \int d\omega_1 d\omega_2 \tilde{G}(\omega_1, \theta^{-1}x_{13})^2 \tilde{G}(\omega_2, \theta^{-1}x_{23})^2 \\ & \times \left[b_3 \rho_F(x_1, t) \rho(x_2, t)_F \rho(x_3, t) + b_4 \rho(x_1, t) \rho(x_2, t) \rho_{FF}(x_3, t) \right. \\ & \left. + b_5 \rho_F(x_1, t) \rho(x_2, t) \rho_F(x_3, t) \right]. \quad (\text{F.2}) \end{aligned}$$

There are many more possibilities in the case of the cubic graph. For simplicity, we will enumerate them in four propagator form, which is obtained after the cancellation of one propagator by the momenta in the numerator of the integrand. There are three combinations of field theory propagators that emerge: the first can be included in Eq. (F.1), the second can be included in Eq. (F.2), and the third is given by

$$\begin{aligned} & \int dt d^{2p}x_1 d^{2p}x_2 d^{2p}x_3 \int d\omega_1 d\omega_2 \tilde{G}(\omega_1, \theta^{-1}x_{12})^2 \tilde{G}(\omega_2, \theta^{-1}x_{23}) \\ & \times \tilde{G}(\omega_1 + \omega_2, \theta^{-1}x_{13}) \left[b_6 \rho_{FF}(x_1, t) \rho(x_2, t) \rho(x_3, t) + b_7 \rho_F(x_1, t) \rho_F(x_2, t) \right. \\ & \left. \times \rho(x_3, t) + b_8 \rho_F(x_1, t) \rho(x_2, t) \rho_F(x_3, t) \right]. \quad (\text{F.3}) \end{aligned}$$

Thus, we can parameterize the inequivalent next to leading order two loop contributions by proportionality constants b_1 through b_8 . Note that by focusing on the constant part of ρ , as we did in the one-loop next to leading order calculation, we obtain two-loop corrections to Eq. (3.17). In particular, the two-loop contribution to the beta function is contained in Eq. (F.3).

Bibliography

- [1] I. Bars and C. Deliduman, Phys. Rev. D **58**, 066004 (1998); I. Bars, C. Deliduman and D. Minic, Phys. Lett. B **457**, 275 (1999).
- [2] N. Seiberg and E. Witten, J. High Energy Phys. **09**, 032 (1999).
- [3] M. M. Sheikh-Jabbari, Phys. Lett. B **455**, 129 (1999); D. Bigatti and L. Susskind, Phys. Rev. D **62**, 066004 (2000); Z. Yin, Phys. Lett. B **466**, 234 (1999); H. Liu and J. Michelson, Phys. Rev. D **62**, 066003 (2000).
- [4] C.P. Martin and D. Sanchez-Ruiz, Phys. Rev. Lett. **83**, 476 (1999); A. Armoni, Nucl. Phys. **B593**, 229 (2001).
- [5] C.P. Martin and F.R. Ruiz, Nucl. Phys. **B597**, 197 (2001).
- [6] T. Krajewski and R. Wulkenhaar, Int. J. Mod. Phys. A **15**, 1011 (2000); I. Chepelev and R. Roiban, J. High Energy Phys. **05**, 037 (2000); H. Girotti, M. Gomes, V. Rivelles and A. da Silva, Nucl. Phys. **B587**, 299 (2000); A. Bichl, *et al*, J. High Energy Phys. **10**, 046 (2000); I. Chepelev and R. Roiban, *ibid.* **03**, 001 (2001); A. Bichl, *et al*, *ibid.* **06**, 013 (2001); S. Sarkar, *ibid.* **06**, 003 (2002).
- [7] S. Minwalla, M. Van Raamsdonk and N. Seiberg, J. High Energy Phys. **02**, 020 (2000).

- [8] M. Hayakawa, Phys. Lett. B **478**, 394 (2000); F.R. Ruiz, *ibid.* **502**, 274 (2001).
- [9] L. Griguolo and M. Pietroni, J. High Energy Phys. **05**, 032 (2001); L. Griguolo and M. Pietroni, Phys. Rev. Lett. **88**, 071601 (2002); G.H. Chen and Y.S. Yu, Nucl. Phys. **B622**, 189 (2002).
- [10] V. V. Khoze and G. Travaglini, J. High Energy Phys. **01**, 026 (2001); T. J. Hollowood, V. V. Khoze and G. Travaglini, *ibid.* **05**, 051 (2001); C. S. Chu, V. V. Khoze and G. Travaglini, Phys. Lett. B **513**, 200 (2001); C. S. Chu, V. V. Khoze and G. Travaglini, *ibid.* **543**, 318 (2002).
- [11] A. Matusis, L. Susskind and N. Toumbas, J. High Energy Phys. **12**, 002 (2000); D. Zanon, Phys. Lett. B **502**, 265 (2001); M. Pernici, A. Santambrogio and D. Zanon, *ibid.* **504**, 131 (2001); A. Santambrogio and D. Zanon, J. High Energy Phys. **01**, 024 (2001).
- [12] Y. Kiem, S. Lee, S. J. Rey and H. T. Sato, Phys. Rev. D **65**, 046003 (2002); Y. Kiem, S. J. Rey, H. T. Sato and J. T. Yee, *ibid.* **65**, 026002 (2002); Y. Kiem, S. Lee, S. J. Rey and H. T. Sato, Eur. Phys. J. **C22**, 757 (2002); Y. Kiem, S. S. Kim, S. J. Rey and H. T. Sato, Nucl. Phys. **B641**, 256 (2002).
- [13] A. Armoni and E. Lopez, Nucl. Phys. **B632**, 240 (2002).
- [14] H. Liu and J. Michelson, Nucl. Phys. **B614**, 279 (2001); H. Liu, *ibid.* **B614**, 305 (2001).

- [15] M. Van Raamsdonk, J. High Energy Phys. **11**, 006 (2001).
- [16] L. Jiang and E. Nicholson, Phys. Rev. D **65**, 105020 (2002).
- [17] E. Nicholson, Phys. Rev. D **66**, 105018 (2002).
- [18] S. Iso, H. Kawai and Y. Kitazawa, Nucl. Phys. **B576**, 375 (2000).
- [19] R. Gopakumar, S. Minwalla and A. Strominger, J. High Energy Phys. **05**, 020 (2000).
- [20] N. Seiberg, J. High Energy Phys. **09**, 003 (2000).
- [21] N. Ishibashi, S. Iso, H. Kawai and Y. Kitazawa, Nucl. Phys. **B573**, 573 (2000); S. J. Rey and R. von Unge, Phys. Lett. B **499**, 215 (2001); S. Das and S. J. Rey, Nucl. Phys. **B590**, 453 (2000); D. Gross, A. Hashimoto and N. Itzhaki, Adv. Theor. Math. Phys. **4**, 893 (2000).
- [22] R. Gopakumar, S. Minwalla, N. Seiberg and A. Strominger, J. High Energy Phys. **08**, 008 (2000).
- [23] A. Rajaraman and M. Rozali, J. High Energy Phys. **04**, 033 (2000).
- [24] S. J. Rey, hep-th/0207108; S. J. Rey and J. T. Yee, hep-th/0303235.

Vita

Eric Alexander Nicholson was born in Hays, Kansas on 17 December 1975, the son of Jack A. Nicholson and Nancy J. Mahr. He received the Bachelor of Science degree in Physics from the Massachusetts Institute of Technology in 1998. He then moved on to the University of Texas at Austin for his graduate studies until 2003. Upon receiving his Ph.D., he plans to join the Department of Defense as an Operations Research Analyst.

Permanent address: 15407 Wild Timber Trail
Cypress, Texas 77433

This dissertation was typeset with \LaTeX^\dagger by the author.

[†] \LaTeX is a document preparation system developed by Leslie Lamport as a special version of Donald Knuth's \TeX Program.